

UNCLASSIFIED

AD NUMBER

ADA800671

CLASSIFICATION CHANGES

TO: unclassified

FROM: secret

LIMITATION CHANGES

TO:
Approved for public release; distribution is unlimited.

FROM:
Distribution authorized to DoD only; Foreign Government Information; MAR 1946. Other requests shall be referred to British Embassy, 3100 Massachusetts Avenue, NW, Washington, DC 20008.

AUTHORITY

DSTL, AVIA 6/12250, 18 Aug 2009; DSTL, AVIA 6/12250, 18 Aug 2009

THIS PAGE IS UNCLASSIFIED

Reproduction Quality Notice

This document is part of the Air Technical Index [ATI] collection. The ATI collection is over 50 years old and was imaged from roll film. The collection has deteriorated over time and is in poor condition. DTIC has reproduced the best available copy utilizing the most current imaging technology. ATI documents that are partially legible have been included in the DTIC collection due to their historical value.

If you are dissatisfied with this document, please feel free to contact our Directorate of User Services at [703] 767-9066/9068 or DSN 427-9066/9068.

**Do Not Return This Document
To DTIC**

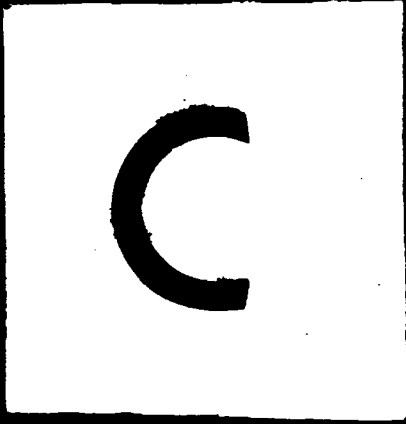
Reproduced by
AIR DOCUMENTS DIVISION



HEADQUARTERS AIR MATERIEL COMMAND

WRIGHT FIELD, DAYTON, OHIO

RFFI



3

6

FRAME

1

0

9

5

NOT SUITABLE FOR FURTHER DISTRIBUTION

TECHNICAL NOTE ARM.344

BRITISH SECRET Equals
UNITED STATES SECRET

ATI No. 1095

SECRET

TECH. REPORT
LOG NO. 551-2-1

TSNTE-6
10 Sept. 46
9/10/46

ROYAL AIRCRAFT ESTABLISHMENT

Farnborough, Hants.

E/AE-TN-ARM.344
E 4760

THE TAIL FORCE SYSTEM ON CAVITATING PROJECTILES

BY

S/LDR. N. SIMMONS M.Sc, Ph. D.

20 JAN 1947

AIR DOCUMENTS DEPARTMENT T-2
AIRCRAFT RESEARCH AND DEVELOPMENT
MICROFILM I.C.
R.C.36 F 1095

ATTENTION IS CALLED TO THE PENALTIES ATTACHING TO ANY INFRINGEMENT OF THE OFFICIAL SECRETS ACT.

THIS DOCUMENT IS THE PROPERTY OF H.M. GOVERNMENT

IT IS INTENDED FOR THE USE OF THE RECIPIENT ONLY, AND FOR COMMUNICATION TO SUCH OFFICERS UNDER HIM AS MAY REQUIRE TO BE ACQUAINTED WITH THE CONTENTS OF THE REPORT IN THE COURSE OF THEIR DUTIES. THE OFFICERS EXERCISING THIS POWER OF COMMUNICATION WILL BE HELD RESPONSIBLE THAT SUCH INFORMATION IS IMPARTED WITH DUE CAUTION AND RESERVE.

ANY PERSON OTHER THAN THE AUTHORISED HOLDER, UPON OBTAINING POSSESSION OF THIS DOCUMENT, BY FINDING OR OTHERWISE, SHOULD FORWARD IT, TOGETHER WITH HIS NAME AND ADDRESS, IN A CLOSED ENVELOPE TO-

THE SECRETARY, MINISTRY OF SUPPLY,
THAMES HOUSE, MILLBANK, LONDON S.W.1

LETTER POSTAGE NEED NOT BE PREPAID; OTHER POSTAGE WILL BE REFUNDED.

ALL PERSONS ARE HEREBY WARNED THAT THE UNAUTHORISED RETENTION OR DESTRUCTION OF THIS DOCUMENT IS AN OFFENCE AGAINST THE OFFICIAL SECRETS ACT 1911-1920.

Mr. Rapp + Bramble
TSNEQ

ENGLISH

LIBRARY

V 53943-EC

SECRET

U.B.R.C. No.53

Tech. Note No. Arm. 344.

March, 1946.

ROYAL AIRCRAFT ESTABLISHMENT, FARNBOROUGH

The Tail Force System on Cavitating Projectiles

- by -

S/Ldr. N. Simmons, M.Sc., Ph.D.

R.A.E. Ref: Arm.S.1345/NS/127.

R.

SUMMARY

Hitherto the complicated problems of the underwater ballistics of long cavitating projectiles have been met only by a conception of steady state motion known as "dynamic equilibrium", associated with trajectories of constant curvature. Yet experiment shows that, except as a first approximation, this simple representation is not sufficient.

The present Note deals with the non-steady motions which actually occur in practice, and the associated variations in lift. In these phenomena, a predominant role is played by the tail forces, and the first requirement is to put these on a quantitative basis. A theoretical method is given which shows how these forces can be accounted for by a "virtual mass" theory, and good agreement is obtained with experimental towing-tank results for the steady planing condition. The theory is readily extendable to more general modes of motion, and the Note demonstrates how it accounts for both stabilising and damping forces.

The development proceeds to the general motion of a cavitating projectile, and it is shown that dynamic equilibrium is achieved only through an "adjustment phase", during the damping-out of the initial oscillation: this phase has a substantial effect on the trajectory. The criteria for stability are also discussed in detail, and it is shown that close agreement is obtained with experiment for such cases as have been investigated practically. The theory also provides the explanation of various effects which have been found to occur in experiment. Preliminary consideration is given to rotated projectiles.

The report provides a basis for future design of underwater projectiles, and for the interpretation of model experiment. In particular it is shown that the adjustment phase can be exploited to give a "skimming trajectory", and proposals are made for tail shaping in suitable cases. Finally it is urged that the body of basic data on nose and tail forces be increased by cavitation tunnel experiment.

V 53943 EC

LIST OF CONTENTS

	Page
1. Introduction	3
2. Virtual mass effect	3
2.1 General considerations	3
2.2 Immersion of an elliptic cylinder	4
2.3 Planing of a circular cylinder	5
3. Determination of virtual mass from experimental results	6
3.1 Examination of lift	6
3.2 Examination of moment	7
3.3 General picture of the force system	7
4. Other modes of motion	9
4.1 Translation	10
4.2 General symmetrical motion	10
4.3 Tail impact	11
5. Trajectory analysis	12
5.1 Dynamic equilibrium	12
5.2 Oscillatory behaviour	19
5.3 Trajectories	25
5.4 Rotated projectiles	29
6. Miscellaneous effects	32
6.1 Effect of tail shape	32
6.2 Residual problems	34
7. Conclusions	34
References	38
Circulation	38

LIST OF TABLES

	Table
Virtual mass and associated functions	I
List of symbols	II

LIST OF ILLUSTRATIONS

	Fig.
Immersion of a general cylinder	1
Immersion of an elliptic cylinder	2
The planing cylinder	3
Virtual mass function	4
Comparison of theoretical and experimental lift	5
Comparison of theoretical and experimental moments	6
Oscillations of a planing cylinder	7
Oscillations of a planing cylinder	8
Force system on a cavitating projectile	9
Dynamic equilibrium: two examples	10
Density correction	11
Dependence of oscillations on C.G. position	12
Oscillations with a forward C.G. position	13
Variation of curvature during the adjustment phase	14
Equilibrium trajectory and actual trajectory	15

1 Introduction

Knowledge of the tail forces on a planing cylinder is essential to two main aspects of the underwater ballistics of cavitating projectiles. First, since such forces provide the bulk of the lift, there is the effect on the curvature of trajectories. Secondly, since such forces are a powerful source of stabilization, there are the effects on dynamic characteristics and on dispersion. The nature and distribution of the tail load are also of importance to design, in connexion with the internal stressing.

Experimental investigation (Ref.1) has provided towing-tank measurements of lift, drag and pitching moment over a range of draughts and incidence. The present study links these results by a theoretical basis and deduces the forces for other modes of motion (viz. vertical entry and rotation). This in turn enables treatment of the problems mentioned above, and the direction of design towards optimum performance. Throughout, the application mainly borne in mind is that to long projectiles which make a shallow entry into water, and travel submerged, at small angles of tail-incidence (up to 10°).

Before proceeding to this, it is necessary to consider how the tail lift force arises. Bearing in mind that the phenomena concerned take place in the tempo of impact on water, we seek the origin of lift partly in a virtual mass effect and partly in the spray formations which as noted in Ref.1 are of considerable importance. Other forces such as buoyancy and surface tension are negligible.

2 Virtual mass effect

2.1 General considerations

The conception of "virtual" or "added" mass arises in classical hydrodynamics in connexion with the motions of completely immersed bodies. It has been extended by a number of writers (see Ref.2) to symmetrical bodies making a vertical entry into water. The form usually assumed for the added mass is the quantity of water contained within an imaginary hemisphere (or semi-cylinder) on the wetted perimeter as base. The variable lift obtained from the imparting of downward momentum to this virtual mass is found to accord well with experimental measurements (Ref.2).

As a starting point for the present investigation, where the relative vertical speeds are of the same order as in impact, the conception of virtual mass is made use of, subject to the proviso that it shall not be regarded as a given quantity, but will be determined from the experimental results.

Consider a horizontal cylinder, of any cross-section symmetrical about a vertical plane (Fig.1), and of maximum width d , which has entered the water with initial speed v_0 and is presently submerged to depth zd with remaining downward velocity v . Then if m be the added mass per unit length of the cylinder and ℓ the lift per unit length derived from the change of momentum of the added mass,

$$\ell = \frac{d}{dt}(mv) = \frac{v^2}{d} \frac{dm}{dz} + \frac{m}{dt} \quad (1)$$

The added volume is a single-valued function of the submergence, so that

maximum for a small value of z , falling away rapidly as z approaches 0.5.

2.3 Planing of a circular cylinder

Consider now a circular cylinder of diameter d planing at constant draught, at constant speed V and angle of incidence α . We define

$$\text{dig-ratio} = \frac{\text{draught}}{\text{diameter}} = \delta \quad (9)$$

The vertical sections are ellipses of the type described in the previous section. At any particular point in the path of the cylinder, the history of the motion is the entry of an elliptic section at speed $V \tan \alpha$ down to a depth δd . It is proposed to apply (6), with the assumption that there is no interference between the flow in successive transverse sections, or, more strictly, that there is no such interference which cannot be allowed for by adjustment of the function $f(z)$. This assumption is made for simplicity in the analysis and its final justification lies in the fact that the form of $f(z)$ will be determined from results of experiments on planing conditions.

Take the origin as the point in the surface vertically above the lowest point of the cylinder (Fig. 3). For the section distant x forward of O , the submergence is $\delta d - x \tan \alpha$, so that

$$z = \delta - \frac{x}{d} \tan \alpha \quad (10)$$

Every section between the origin and the separation point A ($x = \delta d \cot \alpha$) is subject to lift. The lift on sections for which x is negative can easily be verified to be negligible in comparison. Then

$$L = \rho (V \tan \alpha)^2 d \cdot f'(\delta - \frac{x}{d} \tan \alpha) \quad (11)$$

and the total tail lift

$$L_T = \rho V^2 \tan^2 \alpha d \cdot \int_0^{\delta d \cot \alpha} f'(\delta - \frac{x}{d} \tan \alpha) dx$$

i.e.

$$L_T = \rho V^2 d^2 \tan \alpha f(\delta) \quad (12)$$

Also the total moment (positive in the sense of increasing α)

$$M_T = \rho V^2 \tan^2 \alpha d \cdot \int_0^{\delta d \cot \alpha} f'(\delta - \frac{x}{d} \tan \alpha) x dx$$

i.e.

$$M_T = \rho V^2 d^3 f_1(\delta) \quad (13)$$

where

$$f_1(z) = \int_0^z f(z) dz \quad (14)$$

it must be borne in mind that such part of the spray effect, if any, as is expressible in the form $\tan \alpha f(\delta)$, i.e. is equivalent to an addition to the virtual mass, is included in the first term.

Lift calculated from (16) is shown, for typical values of α in Fig. 5, and the experimental values compared. It will be seen that agreement is very close for angles of incidence up to 10° ; there is an indication of agreement at 12° , except that the discontinuity between $\delta = 0.1$ and 0.4 , which is due presumably to some incidental effect, is not revealed. Over the range $\alpha = 0$ to 10° , the present analysis may be applied with confidence; this covers amply the requirements for long underwater projectiles.

3.2 Examination of moment

Formula (13) for the moment about O , together with the values of f_1 given in Table I, enables the virtual mass moment to be calculated. It is still necessary to make allowance for the spray term. In order to do this, values of tail moment were computed from the experimental results of Ref. 1, excluding the small contributions arising from the drag. From these were subtracted values calculated from (13) and it was found that the excess was closely accounted for by addition of a term $0.0160\delta^2 \operatorname{cosec} \alpha$ to $f_1(\delta)$; this represents the effect of spray on moment, so that now

$$M_T = \rho V^2 d^3 \left[f_1(\delta) + 0.0160\delta^2 \operatorname{cosec} \alpha \right] \quad (17)$$

and

$$\text{centre of pressure distance} = \frac{f_1(\delta) + 0.0160\delta^2 \operatorname{cosec} \alpha}{\tan \alpha f(\delta) + 0.0022\delta^2 \operatorname{cosec} \alpha} \cdot d \quad (18)$$

The moment coefficient $M_T / \frac{1}{2} \rho V^2 d^3$ has been graphed in Fig. 6; the experimental values (minus drag contributions) are shown compared with curves computed from (17). It is seen that the agreement is as close as the experimental scatter permits. The small discrepancies remaining are of little importance for our projectile applications, since moments are generally required about centre of gravity positions distant from the tail, and the term M_T is small compared with the contribution from L_T . The centre of pressure distance shows the same general tendencies as the experimental values of Ref. 1. Close agreement is not to be expected here, owing to the critical dependence on measured values. (The figure 1.45 for the C.P. ratio, when $\alpha = 3^\circ$ and $\delta = 0.225$ given in Ref. 1 is a computational error).

3.3 General picture of the force system

We have now obtained a detailed picture of the system of lift forces on a planing cylinder. The bulk of the force can be accounted for by the virtual mass effect. The associated velocity component of lift distribution is

$$c = \rho V^2 \tan^2 \alpha \, d \cdot f' \left(\delta - \frac{x}{d} \tan \alpha \right) \quad (19)$$

leading to total tail lift

$$L_T = \rho V^2 d^2 \tan \alpha f(\delta) \quad (20)$$

and total moment about the trailing edge

$$M_T = \rho V^2 d^3 f_1(\delta) \quad (21)$$

1 Introduction

Knowledge of the tail forces on a planing cylinder is essential to two main aspects of the underwater ballistics of cavitating projectiles. First, since such forces provide the bulk of the lift, there is the effect on the curvature of trajectories. Secondly, since such forces are a powerful source of stabilization, there are the effects on dynamic characteristics and on dispersion. The nature and distribution of the tail load are also of importance to design, in connexion with the internal stressing.

Experimental investigation (Ref.1) has provided towing-tank measurements of lift, drag and pitching moment over a range of draughts and incidence. The present study links these results by a theoretical basis and deduces the forces for other modes of motion (viz. vertical entry and rotation). This in turn enables treatment of the problems mentioned above, and the direction of design towards optimum performance. Throughout, the application mainly borne in mind is that to long projectiles which make a shallow entry into water, and travel submerged, at small angles of tail-incidence (up to 10°).

Before proceeding to this, it is necessary to consider how the tail lift force arises. Bearing in mind that the phenomena concerned take place in the tempo of impact on water, we seek the origin of lift partly in a virtual mass effect and partly in the spray formations which as noted in Ref.1 are of considerable importance. Other forces such as buoyancy and surface tension are negligible.

2 Virtual mass effect

2.1 General considerations

The conception of "virtual" or "added" mass arises in classical hydrodynamics in connexion with the motions of completely immersed bodies. It has been extended by a number of writers (see Ref.2) to symmetrical bodies making a vertical entry into water. The form usually assumed for the added mass is the quantity of water contained within an imaginary hemisphere (or semi-cylinder) on the wetted perimeter as base. The variable lift obtained from the imparting of downward momentum to this virtual mass is found to accord well with experimental measurements (Ref.2).

As a starting point for the present investigation, where the relative vertical speeds are of the same order as in impact, the conception of virtual mass is made use of, subject to the proviso that it shall not be regarded as a given quantity, but will be determined from the experimental results.

Consider a horizontal cylinder, of any cross-section symmetrical about a vertical plane (Fig.1), and of maximum width d , which has entered the water with initial speed v_0 and is presently submerged to depth zd with remaining downward velocity v . Then if m be the added mass per unit length of the cylinder and l the lift per unit length derived from the change of momentum of the added mass,

$$l = \frac{d}{dt}(mv) = v \frac{dm}{dz} + m \frac{dv}{dt} \quad (1)$$

The added volume is a single-valued function of the submergence, so that

$$m = \rho d^2 f(z) \quad (2)$$

where ρ is the density of water, and $f(z)$ is a function to be determined.

Then

$$\ell = \rho v^2 d \cdot f'(z) + \rho d^2 \frac{dv}{dt} f(z) \quad (3)$$

so that the lift consists of two parts:-

- (1) dependent on the instantaneous value of v ; this will be referred to as the velocity component:
- (2) dependent on the instantaneous value of $\frac{dv}{dt}$; this will be referred to as the acceleration component.

For the case in which the cylinder is falling freely under its own weight, we have the additional equation

$$M \frac{dv}{dt} = Mg - \ell \quad (4)$$

where M is the mass of the cylinder per unit length: then

$$\ell = \frac{\rho v^2 d \cdot f' + \rho d^2 g f}{1 + \frac{\rho d^2 f}{M}} \quad (5)$$

Again for the case of constrained entry at constant speed,

$$\ell = \rho v^2 d \cdot f'(z) \quad (6)$$

The form of $f(z)$ depends on the shape of the cylinder.

2.2 Immersion of an elliptic cylinder

A necessary preliminary to the discussion of planing cylinders is the case of entry of an elliptic cylinder of minor axis d (horizontal) and major axis $d \sec \alpha$ (Fig. 2), constrained to enter at speed v . Then (6) applies, with the appropriate form of $f'(z)$.

The usual assumption of added mass (semi-cylinder) gives

$$f(z) = \frac{\pi}{2} \cos \alpha (z - z^2 \cos \alpha) \quad (7)$$

so that on first contact ($z = 0$),

$$\ell = \frac{\pi \rho}{2} v^2 d \cdot \cos \alpha \quad (8)$$

Since this implies infinite pressure, it is, strictly, impossible, unless in fact the flow is spread by spray over a finite area.

The form of $f'(z)$ to be anticipated from experimental work on impact of spheres (Ref. 2) is a function which attains a pronounced

maximum for a small value of z , falling away rapidly as z approaches 0.5.

2.3 Planing of a circular cylinder

Consider now a circular cylinder of diameter d planing at constant draught, at constant speed V and angle of incidence α . We define

$$\text{dig-ratio} = \frac{\text{draught}}{\text{diameter}} = \delta \quad (9)$$

The vertical sections are ellipses of the type described in the previous section. At any particular point in the path of the cylinder, the history of the motion is the entry of an elliptic section at speed $V \tan \alpha$ down to a depth δd . It is proposed to apply (6), with the assumption that there is no interference between the flows in successive transverse sections, or, more strictly, that there is no such interference which cannot be allowed for by adjustment of the function $f(z)$. This assumption is made for simplicity in the analysis and its final justification lies in the fact that the form of $f(z)$ will be determined from results of experiments on planing conditions.

Take the origin as the point in the surface vertically above the lowest point of the cylinder (Fig. 3). For the section distant x forward of 0, the submergence is $\delta d - x \tan \alpha$, so that

$$z = \delta - \frac{x}{d} \tan \alpha \quad (10)$$

Every section between the origin and the separation point A ($x = \delta d \cot \alpha$) is subject to lift. The lift on sections for which x is negative can easily be verified to be negligible in comparison. Then

$$L = \rho (V \tan \alpha)^2 d \cdot f'(\delta - \frac{x}{d} \tan \alpha) \quad (11)$$

and the total tail lift

$$L_T = \rho V^2 \tan^2 \alpha d \cdot \int_0^{\delta d \cot \alpha} f'(\delta - \frac{x}{d} \tan \alpha) dx$$

i.e.

$$L_T = \rho V^2 d^2 \tan \alpha f(\delta) \quad (12)$$

Also the total moment (positive in the sense of increasing α)

$$M_T = \rho V^2 \tan^2 \alpha d \cdot \int_0^{\delta d \cot \alpha} f'(\delta - \frac{x}{d} \tan \alpha) x dx$$

i.e.

$$M_T = \rho V^2 d^3 f_1(\delta) \quad (13)$$

where

$$f_1(z) = \int_0^z f(z) dz \quad (14)$$

We take the opportunity of defining, in general, for later use,

$$f_n(z) = \int_0^z f_{n-1}(z) dz \quad (n = 1, 2, 3, \dots) \quad (15)$$

With the aid of formulae (12) and (13) we can now turn to the experimental results for lift and moment on planing cylinders and proceed to determine the function f .

3 Determination of virtual mass from experimental results

3.1 Examination of lift

Experimental values of lift on planing cylinders are available, from work done in the R.A.E. towing tank (Ref. 1). The following tabulated values of $L_T/\rho V^2 d^2$ are taken from Fig. 9 of that report:

δ	0.1	0.2	0.3	0.4	0.5	0.6	0.7	0.8
$\alpha = 3^\circ$	0.0049*	0.0091*	0.0139*	0.0185	0.0248	0.0311	0.0381	0.0458
$\alpha = 6^\circ$	0.0120	0.0192	0.0240	0.0282	0.0337	0.0390	0.0450	0.0513
$\alpha = 10^\circ$	0.0209	0.0308	0.0373	0.0442	0.0510	0.0573	0.0643	0.0709

These figures do not show the simple proportionality to $\tan \alpha$ indicated by (12): lifts for small angles of incidence are relatively too high. The cause for this must be sought in the fact that so far no explicit allowance has been made for the forward blister which accompanies the motion (Ref. 1). The effect of this spray is uncertain and not amenable to analysis, but it is likely to increase with wetted length. Trial and error shows indeed that the discrepancy is accounted for by the term $0.0022 \delta^2 \operatorname{cosec} \alpha$. On subtracting this from the above figures and dividing by $\tan \alpha$, the following results are obtained:

δ	0.1	0.2	0.3	0.4	0.5	0.6	0.7	0.8
$\alpha = 3^\circ$	0.086	0.141	0.193	0.225	0.273	0.305	0.334	0.363
$\alpha = 6^\circ$	0.112	0.174	0.210	0.236	0.270	0.299	0.331	0.356
$\alpha = 10^\circ$	0.118	0.172	0.205	0.238	0.270	0.298	0.329	0.355
Mean	0.105	0.162	0.203	0.233	0.271	0.301	0.331	0.358

Agreement is now quite good, and we adopt these mean values, after slight smoothing, to define the function f . This is graphed with its derivate in Fig. 4: its values over the range $\delta = 0$ to 1 are shown in Table I, which also gives the values of the functions f_1 , f_2 etc., as found by numerical integration.

With f and f' so defined, the formula for lift becomes

$$L_T = \rho V^2 d^2 \left[\tan \alpha f(\delta) + 0.0022 \delta^2 \operatorname{cosec} \alpha \right] \quad (16)$$

The second term will be referred to as the spray component, though

* Interpolated values.

it must be borne in mind that such part of the spray effect, if any, as is expressible in the form $\tan \alpha f(\delta)$, i.e. is equivalent to an addition to the virtual mass, is included in the first term.

Lift calculated from (16) is shown, for typical values of α in Fig. 5, and the experimental values compared. It will be seen that agreement is very close for angles of incidence up to 10° ; there is an indication of agreement at 12° , except that the discontinuity between $\delta = 0.1$ and 0.4 , which is due presumably to some incidental effect, is not revealed. Over the range $\alpha = 0$ to 10° , the present analysis may be applied with confidence; this covers amply the requirements for long underwater projectiles.

3.2 Examination of moment

Formula (13) for the moment about O, together with the values of f_1 given in Table I, enables the virtual mass moment to be calculated. It is still necessary to make allowance for the spray term. In order to do this, values of tail moment were computed from the experimental results of Ref. 1, excluding the small contributions arising from the drag. From these were subtracted values calculated from (13) and it was found that the excess was closely accounted for by addition of a term $0.0160\delta^2 \operatorname{cosec} \alpha$ to $f_1(\delta)$; this represents the effect of spray on moment, so that now

$$M_T = \rho V^2 d^3 \left[f_1(\delta) + 0.0160\delta^2 \operatorname{cosec} \alpha \right] \quad (17)$$

and

$$\text{centre of pressure distance} = \frac{f_1(\delta) + 0.0160\delta^2 \operatorname{cosec} \alpha}{\tan \alpha f(\delta) + 0.0022\delta^2 \operatorname{cosec} \alpha} \cdot d \quad (18)$$

The moment coefficient $M_T / \frac{1}{2} \rho V^2 d^3$ has been graphed in Fig. 6: the experimental values (minus drag contributions) are shown compared with curves computed from (17). It is seen that the agreement is as close as the experimental scatter permits. The small discrepancies remaining are of little importance for our projectile applications, since moments are generally required about centre of gravity positions distant from the tail, and the term M_T is small compared with the contribution from L_T . The centre of pressure distance shows the same general tendencies as the experimental values of Ref. 1. Close agreement is not to be expected here, owing to the critical dependence on measured values. (The figure 1.45 for the C.P. ratio, when $\alpha = 3^\circ$ and $\delta = 0.225$ given in Ref. 1 is a computational error).

3.3 General picture of the force system

We have now obtained a detailed picture of the system of lift forces on a planing cylinder. The bulk of the force can be accounted for by the virtual mass effect. The associated velocity component of lift distribution is

$$l = \rho V^2 \tan^2 \alpha \, d \cdot f' \left(\delta - \frac{x}{d} \tan \alpha \right) \quad (19)$$

leading to total tail lift

$$L_T = \rho V^2 d^2 \tan \alpha f(\delta) \quad (20)$$

and total moment about the trailing edge

$$M_T = \rho V^2 d^3 f_1(\delta) \quad (21)$$

There is also a spray effect which, according to our approximate analysis, results in the addition of a term $\rho V^2 d^2 (0.00225^2 \text{ cosec } \alpha)$ to the total lift and $\rho V^2 d^3 (0.01606^2 \text{ cosec } \alpha)$ to the total moment. We have no information on the distribution of this effect, but it will appear that this is unnecessary for projectile applications. It must be emphasized that the spray corrections quoted are most probably not correct even in mathematical form, but are merely roughly fitted to the experimental data in order to obtain some quantitative measure of the effect. They do indicate that the relative magnitudes of lift and moment corrections are such that there must be both positive and negative spray lift over the wetted area.

Now the spray pattern is subject to a severe scale effect. It is shown in Ref. 1 that at a certain critical speed the forward blister breaks away completely. Certainly in the applications which are the concern of the present Note, such extensive spray is not observed. The circumstance of reduced pressure in the cavity assists the break-away process in two ways: first, directly, by bringing the entire spray nearer to the cavitation point; secondly, since the free streamlines are isotachs of a speed slightly in excess of the relative speed of the body to the water, the spray is moving faster, and there is a larger radial pressure drop on account of the increased centrifugal force; but this is a small effect. Hence it is very probable that, for the applications in mind, the forward blister which proved so troublesome in the towing tank experiments is absent. In what follows, the spray term is therefore neglected. This does not however entirely dispose of the matter, since as noted above, it is possible that the blister may act, in part, to increase the virtual mass term. If this should be so, we have no means here to disentangle the true virtual mass component from the added term which, although valid in the towing tank, would be irrelevant to cavitating projectiles. The best way to obtain unquestionable values for the virtual mass function is by cavitation tunnel experiment, but this is not yet possible. Our present procedure, though not as infallible as could be wished, is the only possible one in the circumstances. The close agreement with experimental results for cavitating projectiles, which appears later (see 5.1) indicates that our procedure is more reliable than might be expected.

Further experiment would be necessary to settle whether $f(\delta)$ changes appreciably with much increased speed: the suggestion of Ref. 1 to this effect is strongly endorsed. Meanwhile we can only assume that $f(\delta)$ does not change appreciably (as theory indicates), and the further analysis proceeds on this basis.

We are now in a position to consider the acceleration component of lift, where the speed of the projectile is not constant. With the aid of (3), this seen to be

$$l = \rho \frac{dV}{dt} \tan \alpha d^2 f(\delta - \frac{x}{d} \tan \alpha) \quad (22)$$

The corresponding total lift and moment are easily found:-

$$\left. \begin{aligned} L_T &= \rho \frac{dV}{dt} d^3 f_1(\delta) \\ M_T &= \rho \frac{dV}{dt} d^4 \cot \alpha f_2(\delta) \end{aligned} \right\} \quad (23)$$

It is not part of the present object to study the drag forces

For projectile applications, α is small enough for these formulae to be simplified as follows:-

Velocity component:-

$$\left. \begin{aligned} \ell &= \rho(U + V\alpha)^2 d.f'(\delta - \frac{x}{d}\alpha) \\ L_T &= \rho(U + V\alpha)^2 \frac{d^2}{\alpha} f(\delta) \\ M_T &= \rho(U + V\alpha)^2 \frac{d^3}{\alpha^2} f_1(\delta) \quad * \\ \text{C.P. distance} &= \frac{f_1(\delta)}{f(\delta)} \frac{d}{\alpha} \quad * \end{aligned} \right\} \quad (27)$$

Acceleration component:

$$\left. \begin{aligned} \ell &= \rho \left(\frac{dU}{dt} + \frac{dV}{dt} \alpha \right) d^2.f(\delta - \frac{x}{d}\alpha) \\ L_T &= \rho \left(\frac{dU}{dt} + \frac{dV}{dt} \alpha \right) \frac{d^3}{\alpha} f_1(\delta) \\ M_T &= \rho \left(\frac{dU}{dt} + \frac{dV}{dt} \alpha \right) \frac{d^4}{\alpha^2} f_2(\delta) \quad * \\ \text{C.P. distance} &= \frac{f_2(\delta)}{f_1(\delta)} \frac{d}{\alpha} \quad * \end{aligned} \right\} \quad (28)$$

The function $f_1(\delta)/f(\delta)$ is given in Table I.

Substitution of representative values for projectiles shows that in general the acceleration effects are small compared with the velocity effects.

4.2 General symmetrical motion

Suppose now that in addition to the translatory velocities U , V , of the trailing edge, the body has angular velocity Ω in the pitching plane (measured positively in the sense of increasing pitch). Then at the section distant x forward of the trailing edge, the effective downward velocity is $U + V\alpha - \Omega x$.

Thus, for the velocity component,

$$\left. \begin{aligned} \ell &= \rho \left[(U+V\alpha)^2 - 2(U+V\alpha)\Omega x + \Omega^2 x^2 \right] d.f'(\delta - \frac{x}{d}\alpha) \\ L_T &= \rho(U+V\alpha)^2 \frac{d^2}{\alpha} f(\delta) - 2\rho(U+V\alpha)\Omega \frac{d^3}{\alpha^2} f_1(\delta) + 2\rho\Omega^2 \frac{d^4}{\alpha^3} f_2(\delta) \\ M_T &= \rho(U+V\alpha)^2 \frac{d^3}{\alpha^2} f_1(\delta) - 4\rho(U+V\alpha)\Omega \frac{d^4}{\alpha^3} f_2(\delta) + 6\rho\Omega^2 \frac{d^5}{\alpha^4} f_3(\delta) \end{aligned} \right\} \quad (29)$$

while, for the acceleration component,

* $x \frac{16}{15}$ if the drag contribution be approximately allowed for.

on tails, since such forces play only a minor role in the problems to be discussed: owing to the preponderance of nose drag, and for other reasons, it is sufficient to regard the retardation of an underwater projectile as being strictly proportional to V^2 , the constant of proportionality being independent of pitch. The only way in which we shall be concerned with tail drag is in respect of the small contribution it makes to the total tail moment about the centre of gravity (see Fig. 9). For this purpose a rough approximation will suffice: this is provided by the results of Ref. 1, in which we note that the drag/lift ratio is approximately independent of δ , but varies with α , as follows

α	3°	6°	10°
drag/lift	1.3	0.6	0.4

which can be fitted by

$$D_T = \frac{L_T}{15\alpha} \quad (24)$$

This relation implies that the moment of tail drag about a distant point in the projectile is 1/15th of that due to tail lift, so that drag can be sufficiently allowed for hereafter by multiplying moments due to lift by the factor 16/15.

4 Other modes of motion

4.1 Translation

A general translatory motion of the cylinder involves a downward velocity U in addition to the forward velocity V (lateral motions excluded). Then each vertical section has effective downward velocity $U + V \tan \alpha$, and the results of (3.3) apply provided we replace $V \tan \alpha$ by the new expression. Then, for the velocity component,

$$\left. \begin{aligned} \ell &= \rho(U + V \tan \alpha)^2 d \cdot f'(\delta - \frac{x}{d} \tan \alpha) \\ L_T &= \rho(U + V \tan \alpha)^2 d^2 \cot \alpha f(\delta) \\ M_T &= \rho(U + V \tan \alpha)^2 d^3 \cot^2 \alpha f_1(\delta) \\ \text{C.P. distance} &= \frac{f_1(\delta) \cdot d \cot \alpha}{f(\delta)} \end{aligned} \right\} \quad (25)$$

and for the acceleration component,

$$\left. \begin{aligned} \ell &= \rho \left(\frac{dU}{dt} + \frac{dV}{dt} \tan \alpha \right) d^2 \cdot f \left(\delta - \frac{x}{d} \tan \alpha \right) \\ L_T &= \rho \left(\frac{dU}{dt} + \frac{dV}{dt} \tan \alpha \right) d^3 \cot \alpha f_1(\delta) \\ M_T &= \rho \left(\frac{dU}{dt} + \frac{dV}{dt} \tan \alpha \right) d^4 \cot^2 \alpha f_2(\delta) \\ \text{C.P. distance} &= \frac{f_2(\delta)}{f_1(\delta)} \cdot d \cot \alpha \end{aligned} \right\} \quad (26)$$

* $\times \frac{16}{15}$ if the drag contribution be approximately allowed for.

$$\begin{aligned}
 \ell &= \rho \left(\frac{dU}{dt} + \frac{dV}{dt} \alpha - \frac{d\Omega}{dt} x \right) d^2 \cdot f(\delta - \frac{x}{d} \alpha) \\
 L_T &= \rho \left(\frac{dU}{dt} + \frac{dV}{dt} \alpha \right) \frac{d^3}{\alpha} f_1(\delta) - \rho \frac{d\Omega}{dt} \frac{d^4}{\alpha^2} f_2(\delta) \\
 M_T &= \rho \left(\frac{dU}{dt} + \frac{dV}{dt} \alpha \right) \frac{d^4}{\alpha^2} f_2(\delta) - 2\rho \frac{d\Omega}{dt} \frac{d^5}{\alpha^3} f_3(\delta)
 \end{aligned} \quad (30)$$

In underwater ballistic applications, the angular velocity and acceleration terms are generally small.

4.3 Tail impact

Consider now a cylinder of mass M , diameter d and length Ld , impacting on water at angle of inclination α . In order to simplify the mathematics and enable the fundamentals of the motion to be more readily appreciated, it will be assumed that, during impact, a vertical force is applied at the front end of the cylinder of such a magnitude as to ensure that α remains unchanged throughout. This is a rather artificial device, which divorces the case from practical applications, but it does help in elucidating the basic characteristics of the impact motion.

If the relative horizontal speed of cylinder and water be V , the tail lift is given by

$$L_T = \rho (\dot{\delta}d + V\alpha)^2 \frac{d^2}{\alpha} f(\delta) \quad (31)$$

the initial value $\dot{\delta}_0$ being arbitrary. The nose lift L_N follows from the consideration that moments about the trailing edge must balance, so that

$$L_N = - \frac{\rho}{L} (\frac{\dot{\delta}d}{\alpha} + V)^2 d^2 f_1(\delta) \quad (32)$$

The equation of vertical motion is then

$$\sigma \alpha^2 \ddot{\delta} = (\dot{\delta} + \frac{V\alpha}{d})^2 \left[\frac{1}{L} f_1(\delta) - \alpha f(\delta) \right] \quad (33)$$

where

$$\sigma = \frac{M}{\rho d^3} \quad (34)$$

the specific gravity coefficient. The solution of this equation is readily obtained by standard methods as

$$\begin{aligned}
 \log \left(1 + \frac{\dot{\delta}d}{V\alpha} \right) + \left(1 + \frac{\dot{\delta}d}{V\alpha} \right)^{-1} + \frac{f_1(\delta)}{\sigma \alpha} - \frac{f_2(\delta)}{\sigma \alpha^2 L} \\
 = \log \left(1 + \frac{\dot{\delta}_0 d}{V\alpha} \right) + \left(1 + \frac{\dot{\delta}_0 d}{V\alpha} \right)^{-1}
 \end{aligned} \quad (35)$$

When $\delta = 0$, (35) gives

$$\log \left(1 + \frac{\dot{\delta}d}{V\alpha} \right) + \left(1 + \frac{\dot{\delta}d}{V\alpha} \right)^{-1} = \log \left(1 + \frac{\dot{\delta}_0 d}{V\alpha} \right) + \left(1 + \frac{\dot{\delta}_0 d}{V\alpha} \right)^{-1} \quad (36)$$

of which the solution $\dot{\delta} = \dot{\delta}_0$ corresponds to entry: the other

solution, which gives a negative value of δ and corresponds to exit, may easily be obtained by the aid of an auxiliary graph of the expression $\log(1+x) + (1+x)^{-1}$. The maximum value of δ is given by

$$1 + \frac{f_1(\delta)}{\sigma \alpha} - \frac{f_2(\delta)}{\sigma \alpha^2 L} = \log\left(1 + \frac{\delta_{od}}{V\alpha}\right) + \left(1 + \frac{\delta_{od}}{V\alpha}\right)^{-1} \quad (37)$$

Further, for any particular case, when δ_0 , V , d , α , σ , L are known, δ can be plotted for the entire period of immersion with the aid of the auxiliary graph, and the behaviour (δ , t relation, accelerations, etc.) deduced.

By way of illustration, we have taken the case where $M = 1000$ lbs., $d = 0.85$ ft., $L = 10.4$, $\sigma = 26.1$, $\alpha = 0.07$ rad. corresponding roughly to the rocket projectile "Uncle Tom", and with $\delta_0 d/V\alpha = 0.25, 0.50, 0.75$. The values of $\delta d/V\alpha$ obtained from (35) are plotted in Fig. 7. The graphs show that the trailing edge enters to a depth which increases rapidly with entry velocity, rebounds, and finally emerges with considerably reduced speed. In all cases, powerful lifting forces are invoked, with substantial damping.

For the reason explained above, these results are not directly applicable to the tail impact of a projectile on its cavity wall, where there is appreciable rotation of the body, and moreover the curvature of the trajectory implies a centrifugal force tending to stabilize the cylinder at a dig-ratio greater than zero. Nevertheless it has been thought worth while to develop one of the cases of Fig. 7. to a complete solution. The case $\delta_0 d/V\alpha = 0.5$ has been selected and the δ , t relation deduced by numerical evaluation of

$$t = \int_0^{\delta} \frac{d \delta}{\delta} \quad (38)$$

Graphs of δ and δ/V against Vt for this case are shown in Fig. 8. It is seen that δ decays to 0.575 of its initial value in the "half-period" of immersion, and that both frequency and damping constant increase proportionally with V . The maximum value of δ is $0.0011 V^2$, amounting, at 900 f/s, to 28g. This is of the same order as that indicated in tank firings of models.

An analysis which takes account of projectile rotation and trajectory curvature is given in the following sections.

5 Trajectory analysis

5.1 Dynamic equilibrium

The notion of "dynamic equilibrium" was introduced by Blackwell (Ref. 3) in order to give a simple explanation of the underwater behaviour of rockets. It is a state in which the projectile moves at constant pitch and dig-ratio, in a path which would, apart from gravity effect, have constant upward curvature, the nose and tail forces providing a couple just sufficient to account for the rotation of the projectile due to trajectory curvature; he shows that, to a sufficient order of approximation, these forces may be regarded as balancing statically about the centre of gravity.

Though motion of this type is not conformed with in practice,

the conception does provide a very useful basis on which to build an investigation of the actual motions. We set out here to study dynamic equilibrium in a more complete manner, in the light of the closer representation of the tail form system which has been developed above.

Consider then a long cylinder, of diameter d and length Ld , maintained in cavitating motion with tail incidence α and dig-ratio δ (Fig. 9). It is presumed that L is great enough for the nose and tail forces to be considered as two separate systems and that Ld is measured to the centre of pressure of nose forces (assumed, with sufficient accuracy, to be a fixed point). Let z denote the centre of gravity ratio viz. the distance from nose C.P. to the centre of gravity, divided by total length Ld .

It will be assumed, with Blackwell, that cavity shape over the region of tail contact, and cavitation number, are independent of the attitude of the projectile, provided the pitch angle is, as here, small. Then the cavity is, presumably, symmetrical with respect to the path of the nose (Fig. 9). These assumptions are reasonable enough for the present state of underwater ballistics, but the future is likely to demand that the laws of cavity behaviour should be studied in detail, so that a closer representation, if necessary, may be obtained. With the assumptions, it is permissible to imagine the round pivoting about the nose centre of pressure, so that

$$\delta = L (\alpha - \beta) \quad (39)$$

where β is the value of α at which tail contact is first made; further, owing to the irrelevance of cavity pressure, the results of (4.1) may be applied. The effect of the transverse curvature of the cavity is ignored (see 6.2).

Then, putting $U = 0$ in (27), we obtain for the tail system

$$\left. \begin{aligned} L_T &= \rho V^2 d^2 a f(\delta) \\ M_T &= \rho V^2 d^3 f_1(\delta) \frac{16}{15} \end{aligned} \right\} \quad (40)$$

Hence the tail moment about the centre of gravity is

$$M_T^G = \frac{16}{15} \rho V^2 d^3 \left[f_1(\delta) - (\delta + L\beta)(1-z)f(\delta) \right] \quad (41)$$

Next we must give some consideration to the nose system. Apart from a few drag measurements, these forces have had no direct experimental investigation in this country. The method of integration of wind tunnel pressure plots has however been carried out for a few nose shapes (see Ref. 3), and although these figures are not likely to be reliable, we make use of them as the only available data. For our purpose, it is sufficient to note that for a long body placed at rest at angle of pitch i in a uniform infinite stream of general speed V , the nose force can be resolved into an axial component, independent of i for small angles of pitch, and a transverse force, in the sense such as to increase pitch (assuming we have a lift-producing shape): over the practical range of cavitation numbers (0 - 0.02 and possibly up to 0.05), this transverse force is expressible as

$$L_N = \frac{1}{2} \rho V^2 d^2 \nu i \quad (42)$$

where ν is a characteristic constant for the head shape. The following results are adapted from Ref. 3:-

$$\begin{array}{ll} \text{Full cone, } 45^\circ & \nu = 0.63 \\ \text{Full cone, } 75^\circ & \nu = 0.40 \\ \text{Ogive, 1.4 c.r.h.} & \nu = 0.37 \end{array} \quad (43)$$

The values for reduced heads diminish as the square of the diameter. In the future it should be possible to get more reliable figures from cavitation tunnel experiment; in the mean-time we use estimates based on the above.

For the nose moment about the centre of gravity, since the forward wetted area is concentrated, and at a considerable distance,

$$M_N^1 = \frac{1}{2} \rho V^2 d^3 L_z \nu i. \quad (44)$$

Now the angle of incidence at the nose differs from that at the tail since the cavity surface at the rear is inclined to the axis of the cavity (direction of motion) at an angle γ (Fig. 9).

Furthermore, the angle of incidence at the nose is, in effect, reduced by the rotation of the projectile about its centre of gravity by amount $L_z \delta$, where c is the upward curvature of the path of the centre of gravity. Hence

$$i = \alpha + \gamma - L_z \delta \quad (45)$$

The angle γ will, ultimately be obtainable from an adequate theory of cavities, and must meantime be estimated: c is calculable in terms of the total lift force, and mass and speed of the projectile. In practical cases $L_z \delta$ is of the order of 0.01 while $(\alpha + \gamma)$ is of the order 0.1 and z is of the order 0.5, so that the last term in (45) is in the nature of a small correction. Then for the nose lift and moment about the centre of gravity, we may write

$$\begin{aligned} L_N &= \frac{1}{2} \rho V^2 d^2 \nu (\alpha + \gamma - L_z \delta) \\ M_N^1 &= \frac{1}{2} \rho V^2 d^3 L_z \nu (\alpha + \gamma - L_z \delta) \\ &= \frac{1}{2} \rho V^2 d^3 z \nu (\delta + L_\delta + L_\gamma - L^2 z \delta) \end{aligned} \quad (46)$$

The equation of normal motion is then, assuming the trajectory inclination to the horizontal small enough for neglect of cosine effects,

$$\sigma (V^2 c + g) = \frac{L_T + L_N}{\rho d^3} = \frac{V^2}{d} \left[\alpha f(\delta) + \frac{1}{2} \nu (\alpha + \gamma - L_z \delta) \right] \quad (47)$$

where σ is the specific gravity coefficient, as defined in (34), and not to be confused with the average specific gravity. Hence

SECRET

Tech. Note No. Arms 344.

$$L\bar{c} = \frac{(\bar{\delta} + L\beta)f(\bar{\delta}) + \frac{1}{2}\nu(\bar{\delta} + L\beta + LY) - L\sigma g/\nu^2}{\sigma + \frac{1}{2}\nu Lz} \quad (48)$$

giving the equilibrium curvature \bar{c} in terms of $\bar{\delta}$, the equilibrium dig-ratio, and known constants. If we define a gravity correction by

$$G = \frac{L\sigma g}{\nu^2} \frac{1}{(\bar{\delta} + L\beta)f(\bar{\delta}) + \frac{1}{2}\nu(\bar{\delta} + L\beta + LY)} \quad (49)$$

we have the alternative form

$$L\bar{c} = \left[(\bar{\delta} + L\beta) f(\bar{\delta}) + \frac{1}{2}\nu(\bar{\delta} + L\beta + LY) \right] \frac{(1-G)}{\sigma + \frac{1}{2}\nu Lz} \quad (50)$$

This equation enables \bar{c} to be calculated when $\bar{\delta}$ is known, and vice versa.

The equation of rotational motion is, as noted above.

$$M' \equiv M'_T + M'_N = 0 \quad (51)$$

so that

$$\left[f_1(\bar{\delta}) - (\bar{\delta} + L\beta)(1-z)f(\bar{\delta}) \right] + \frac{15}{32}\nu z \left[\bar{\delta} + L\beta + LY - L^2z\bar{c} \right] = 0 \quad (52)$$

To exhibit the dependence of \bar{c} on z , we bear in mind that the term involving \bar{c} is a small one, and solve first with $\bar{c} = 0$ (corresponding to a projectile whose density is such that the weight exactly balances the total lift): we then obtain directly

$$z_{\infty} = \frac{(\bar{\delta} + L\beta)f(\bar{\delta}) - f_1(\bar{\delta})}{(\bar{\delta} + L\beta)f(\bar{\delta}) + \frac{15}{32}\nu(\bar{\delta} + L\beta + LY)} \quad (53)$$

Then, for the general case, the solution can be found by simple algebraic approximation as

$$z = z_{\infty} + \frac{15 z_{\infty}^2}{\frac{32\sigma}{\nu L} - 14 z_{\infty}} \quad (54)$$

if, as is generally the case in underwater ballistic applications, the velocity is high, or more generally,

$$z = z_{\infty} + \frac{15 z_{\infty}^2 (1-G)}{\frac{32\sigma}{\nu L} - z_{\infty}(14-30G)} \quad (55)$$

The added term, to which we shall allude as the "density correction", is small: its magnitude is such that correcting terms of higher order need never, in practical cases, be considered. In fact, the density correction is really of importance only when z_{∞} is near its critical value (see below).

Equations 50, 53, 55 provide all necessary information concerning dynamic equilibrium. The last two enable dig-ratio to be calculated for any given centre of gravity position, and the first then enables trajectory curvature to be deduced. It is found that the theoretical results obtained in this way agree very closely with such experimental data as are available.

In order to elucidate the properties of relations (53) and (54) we have plotted in Fig. 10 and $\bar{\delta}$, z_{∞} relation for two examples of practical importance: these are average Uncle Tom shapes (reduced cone noses) of lengths 10 and 15 diameters respectively. The values of the constants taken were

$$(i) L = 10, \nu = 0.25, I_{\beta} = 0.36, LY = 0.12$$

$$(ii) L = 15, \nu = 0.25, I_{\beta} = 0.48, LY = 0.12$$

The values of β and γ were obtained by measurement of G.F.R.S. arditron photographs of cavities: the value of ν was estimated from (43). The graph shows $\bar{\delta}$ as a function of z_{∞} ; the $\bar{\delta}$, z relation can be obtained by applying the density correction given in Fig. 11 for the appropriate value of $2\sigma/L\nu$. (The density correction for case (ii) is not shown - the values are 50% greater than those for case (i)).

It is apparent from Fig. 10 that a critical value z^* exists: if z exceeds this, dynamic equilibrium is impossible: for the 10 diameter case, $z^* = 0.436$; for the 15 diameter case, $z^* = 0.472$. While z remains appreciably smaller than z^* , $\bar{\delta}$ is a single-valued function of z and so a single projectile attitude corresponds to a given centre of gravity position. But as z approaches its critical value, $\bar{\delta}$ increases very steeply; theoretically, when z is nearly critical, there is a second solution for $\bar{\delta}$; in practice $\bar{\delta}$ is indeterminate. Similar properties are evidenced by the dynamic equilibrium curve, for all practicable values of the constants.

The existence of a dynamic equilibrium position is a necessary (though not sufficient) condition for the stability of a long underwater projectile, in the loose sense that, unless such a position exists, the pitch will increase indefinitely. The condition

$$z < z^* = z_{\infty}^* + \frac{15(z_{\infty}^*)^2}{\frac{32\sigma}{\nu L} = 14z_{\infty}^*} \quad (56)$$

where z_{∞}^* is the maximum value of z_{∞} shown on the $\bar{\delta}$, z_{∞} graph, may therefore be adopted as a practical criterion of stability. The figures given above for z^* in the case of the two Uncle Tom models agree very closely with those deduced from G.F.R.S. experiments (Ref. 4) and thereby afford quantitative verification of the force system we have employed, and especially of the procedure criticised in (3.3). It must be remembered in this connexion that z here is measured from the nose centre of pressure: practical values measured from the tip of the projectile are up to 0.025 greater.

The position of dynamic equilibrium is easily proved to be always statically stable: if there are two positions, this applies to the one of small dig-ratio. For the total static moment M' is positive at $\bar{\delta} = 0$ (restricting ourselves to lift-producing shapes), and zero at $\bar{\delta} = \bar{\delta}$; thus $\frac{\partial M'}{\partial \bar{\delta}}$ must be negative at $\bar{\delta}$, though small. The possibility of neutral stability is ruled out because $\frac{\partial^2 M'}{\partial \bar{\delta}^2}$ can

easily be shown to be positive, up to the critical position. By the same token, if z is nearly critical and a second position of dynamic equilibrium exists, it will be statically unstable. If, owing to high initial angular velocity, the tail passes this second position, the round will turn to large angles of pitch.

The plotted examples (Fig.10) show that when z is fixed, stability may be increased by lengthening the projectile, or alternatively that longer projectiles can be stabilized with greater C.G. ratios: this is a well-known experimental effect (Ref.4). Another, but less important, effect is that of projectile density. This does not influence z_{co}^* , but it does affect the density correction. In practical cases this is only of order 0.01 or 0.02, but if an assigned shape be given an artificially low density, the correction will take on a very inflated value, and substantially increase the critical C.G. ratio. This effect has been observed in experiment; thus Duncan (Ref.5) found that an unduly light projectile with the following characteristics:

$$L = 10, \quad z = 0.47 \text{ (from tip), specific gravity } 0.58 \\ \text{nose } 30^\circ \text{ cone (estimated } \nu = 0.8);$$

was stable, but that a projectile of about six times this specific gravity and otherwise identical, was quite unstable. In Fig.11 are plotted the correction curves (iii) for the heavy projectile ($2\sigma/L\nu = 8.5$) and (iv) for the light projectile ($2\sigma/L\nu = 1.28$). It is quite evident that here the light projectile is stabilized by the abnormally high density-correction. However, such a bonus is not available to the designer of high speed underwater weapons, for which the density must normally be high, although the advantage would be secured with projectiles of the torpedo type.

It may be noted that, apart from the small gravity effect, the position of dynamic equilibrium is independent of speed V ; but although the actual value of V is irrelevant, it is assumed that the value chosen is maintained constant. On the actual trajectory, we have retardation proportional to the square of speed: hence even though \bar{c} remains constant, the angular velocity of the projectile decreases, and the equations of normal and angular motion are affected. This is easily allowed for as a modification of the preceding analysis, as follows.

Let h be the travel parameter appropriate to the retardation, so that

$$\frac{dV}{dt} = -\frac{V^2}{h} \quad (57)$$

In any position of dynamic equilibrium, neglecting the small gravity effect, \bar{c} must remain constant: hence

$$\text{angular acceleration} = \frac{d}{dt} (V\bar{c}) = -\frac{V^2\bar{c}}{h} \quad (58)$$

Then if M be the mass of the projectile and nl its transverse radius of gyration about the centre of gravity, the inertial term $-Mn^2 d^2 V^2 \bar{c} / h$ must appear on the right hand side of (51). This equation must also be modified so as to include the acceleration terms from (4.1). We do not give the algebraic details here, but the results are as follows. The formula for z_{co} is unchanged, but the density correction is modified so that now

$$z - z_{\infty} = \frac{15(z_{\infty}^2 - \frac{2\alpha n^2 d}{\nu h L^2})(1-G-H) + 16(\frac{2\sigma}{\nu L} + z_{\infty})H'}{(\frac{32\sigma}{\nu L} + 16z_{\infty})(1-H) - 30z_{\infty}(1-G-H) - 16H'} \quad (59)$$

where

$$H = \frac{Ld}{h} \frac{r_1(\bar{\delta})}{(\bar{\delta} + L\beta)f(\bar{\delta}) + \frac{15\nu}{32}(\bar{\delta} + L\beta + L\gamma)} \quad (60)$$

and

$$H' = \frac{Ld}{h} \frac{f_2(\bar{\delta}) - (\bar{\delta} + L\beta)(1-z)f_1(\bar{\delta})}{(\bar{\delta} + L\beta)f(\bar{\delta}) + \frac{15\nu}{32}(\bar{\delta} + L\beta + L\gamma)}$$

A similarly modified value of z^* follows. Thus dynamic equilibrium is still a possible mode of motion under conditions of retardation, and the shifts in the values of $\bar{\delta}$, $\bar{\sigma}$ and z^* are small and calculable.

One assumption that we have tacitly made in the whole of the foregoing analysis deserves mention, viz. that the viscous damping couple associated with the rotation of the body is negligible. We have not taken this into account since no quantitative data are available: it may however be reasonably expected to be small since the cavity rotates with the projectile. It is very desirable that relative data should be obtained from cavitation tunnel experiment in the near future.

We conclude the present section with a few notes on design considerations. Provided that the study of cavities has advanced to the point where it will be possible to assign values of β , γ , ν , which can at the moment only be roughly estimated, one will be able to plot the $\bar{\delta}$, z_{∞} relation (53) for any proposed shape, and determine the value of z_{∞}^* : the necessary corrections can then be applied so as to obtain z^* . The designer however has not discretion to place the centre of gravity so that z is nearly equal to z^* , for there is a sub-critical zone of values of z in which, although the round is stable, it is only just so, the equilibrium dig-ratio is virtually indeterminate, and the lift developed is consequently unpredictable. This is the basic reason why excessive lift requirements are found experimentally to lead to high dispersions.

Thus for reproducible performance, z must fall short of some lower critical value: this point is not easily fixed with precision since it is conditioned by

- (a) the fact that the tail must be prevented by restoring and damping forces from reaching the second equilibrium position, which is virtually indeterminate;
- (b) the necessity for preventing the pitch angle reaching such a magnitude that the projectile makes undesired contact with the cavity at points intermediate between nose and tail;
- (c) the acceptable degree of dispersion, (see 5.3);
- (d) the desirable initial oscillatory characteristics (see 5.2).

Then provided z is made less than the lower critical value, $\bar{\delta}$ will be determinate, and the behaviour predictable. The actual values of

$\bar{\delta}$ and $\bar{\alpha}$ can be obtained by an inverse process: first (54) is solved as a quadratic in z_{∞} giving

$$z_{\infty} = z - \frac{15 z^2}{\frac{32\sigma}{\nu L} - 14 z} \quad (61)$$

(a similar but more general form being obtainable from (59)); then $\bar{\delta}$ is given uniquely by the $\bar{\delta}$, z_{∞} graph, and $\bar{\alpha}$ by (48).

There is, of course, no guarantee that scale effects will not intervene if the values of β and γ are taken from observations on model cavities. A detailed study of cavities both at model and, if possible, at full scale is therefore necessary.

5.2 Oscillatory Behaviour

The considerations of the preceding section are essentially static ones. But a projectile must attain the equilibrium position starting from a state where $\delta = 0$ and reach equilibrium by a more or less damped oscillation; while this is happening, the lift forces vary, with resultant effects on the trajectory. It is necessary therefore for us to consider the oscillatory behaviour of the body. We assume at the outset that the centre of gravity is placed forward of the lower critical position, so that this behaviour is determinate.

These oscillations may conveniently be studied, simultaneously with the stability, as a small perturbation of the (retarded) equilibrium motion, by putting

$$\delta - \bar{\delta} = \varepsilon \quad (62)$$

where ε is small; then

$$\dot{\delta} = \dot{\varepsilon} \quad \ddot{\delta} = \ddot{\varepsilon} \quad \ddot{\alpha} = \frac{\dot{\varepsilon}}{L} \quad (63)$$

Let u denote the corresponding small increment in trajectory curvature, so that

$$\alpha = \bar{\alpha} + u \quad (64)$$

We will use f' , f , f_1 , f_2 , to denote the equilibrium values of corresponding functions: since it is supposed that the analysis of (5.1) has been performed for any given case, $\bar{\delta}$, $\bar{\alpha}$, f' , f , etc. are known constants.

For the present V is taken as constant, neglecting the retardation: this will be justified later. Then the incremental forces and moments to which the projectile is subjected, due to the perturbation of the motion, can be obtained by first-order expansions of (27), (28) and (46); they are:-

Velocity component:

$$\left. \begin{aligned} \Delta L_T &= 2\rho V \cdot d^3 \dot{f}_1 \bar{\epsilon} + \rho V^2 d^2 \left[\frac{f}{L} + \bar{\alpha} f' \right] \bar{\epsilon} \\ \Delta M_T &= \frac{32}{15} \frac{\rho V d^4 \dot{f}_1 \bar{\epsilon}}{\bar{\alpha}} + \frac{16}{15} \rho V^2 d^3 f_1 \bar{\epsilon} \\ \Delta M_T^1 &= \frac{32}{15} \frac{\rho V d^4}{\bar{\alpha}} \left[f_1 - L \bar{\alpha} (1-z) f \right] \bar{\epsilon} + \frac{16}{15} \rho V^2 d^3 \left[z f - L \bar{\alpha} (1-z) f' \right] \bar{\epsilon} \end{aligned} \right\} (65)$$

Acceleration component :

$$\left. \begin{aligned} \Delta L_T &= \frac{\rho d^4}{\bar{\alpha}} f_1 \ddot{\bar{\epsilon}} \\ \Delta M_T &= \frac{16}{15} \frac{\rho d^5}{\bar{\alpha}^2} f_2 \ddot{\bar{\epsilon}} \\ \Delta M_T^1 &= \frac{16}{15} \frac{\rho d^5}{\bar{\alpha}^2} \left[f_2 - L \bar{\alpha} (1-z) f_1 \right] \ddot{\bar{\epsilon}} \end{aligned} \right\} (66)$$

Nose forces:

$$\left. \begin{aligned} \Delta L_N &= \frac{1}{2} \rho V^2 d^2 \frac{v \bar{\epsilon}}{L} - \frac{1}{2} \rho V^2 d^3 v L z u \\ \Delta M_N &= \frac{1}{2} \rho V^2 d^3 v z \bar{\epsilon} - \frac{1}{2} \rho V^2 d^4 v L^2 z^2 u \end{aligned} \right\} (67)$$

Then, for the incremental normal motion,

$$\sigma \rho d^3 v^2 u = \frac{\rho d^4}{\bar{\alpha}} f_1 \ddot{\bar{\epsilon}} + 2 \rho V d^3 \dot{f}_1 \bar{\epsilon} + \frac{\rho V^2 d^2}{L} (f + L \bar{\alpha} f' + \frac{1}{2} v) \bar{\epsilon} - \frac{1}{2} \rho V^2 d^3 v L z u \quad (68)$$

whence

$$L \sigma b \frac{V^2}{d} u = \frac{L}{\bar{\alpha}} f_1 \ddot{\bar{\epsilon}} + 2 L f \frac{V}{d} \dot{\bar{\epsilon}} + (f + L \bar{\alpha} f' + \frac{1}{2} v) \frac{V^2}{d^2} \bar{\epsilon} \quad (69)$$

where for convenience we have written:

$$b = 1 + \frac{v L z}{2 \sigma} \quad (70)$$

In practical cases, $b \approx 1$.

Again the angular velocity = $V_0 + \alpha = V_0 + \bar{\epsilon}/L$, so that the incremental angular acceleration = $V_0 + \ddot{\bar{\epsilon}}/L$ and the equation of incremental rotation reduces to

$$\left. \begin{aligned} \sigma n^2 (v u + \frac{\ddot{\bar{\epsilon}}}{L}) &= \frac{32}{15 \bar{\alpha}} \left[f_1 - L \bar{\alpha} (1-z) f \right] \frac{V}{d} \dot{\bar{\epsilon}} + \frac{16}{15} \left[z f - L \bar{\alpha} (1-z) f' \right] \frac{V^2}{d^2} \bar{\epsilon} \\ &+ \frac{16}{15 \bar{\alpha}^2} \left[f_2 - L \bar{\alpha} (1-z) f_1 \right] \ddot{\bar{\epsilon}} + \frac{1}{2} v z \frac{V^2}{d^2} \bar{\epsilon} - \frac{1}{2} v L z^2 \frac{V^2}{d} u \end{aligned} \right\} (71)$$

In forming this equation, we have, as in the previous section, neglected a small viscous damping term for which there are no

quantitative data available.

The next step is to eliminate u with the aid of (69): this leads to the equation.

$$A\ddot{\varepsilon} + B\frac{V}{d}\dot{\varepsilon} + C\frac{V^2}{d^2}\varepsilon + D\frac{V^3}{d^3}\varepsilon = 0 \quad (72)$$

where

$$\left. \begin{aligned} A &= \frac{n^2 f_1}{a} \\ B &= n^2 \left(2f + \frac{ob}{L} \right) + \frac{L f_1}{15a} (16b - bz - 15z) - \frac{16}{15} \frac{bf_2}{a^2} \\ C &= \frac{n^2}{L} \left(f + L\bar{a}f' + \frac{1}{2}\nu \right) + \frac{2Lf}{15} (16b - bz - 15z) - \frac{32bf_1}{15a} \\ D &= (16b - bz - 15z) \frac{L\bar{a}f'}{15} - \left(1 + \frac{b}{15} \right) z f - \frac{1}{2} \nu z \end{aligned} \right\} \quad (73)$$

Since A is essentially positive, the conditions for dynamic stability are:

$$B, C, D > 0 \quad BC - AD > 0 \quad (74)$$

It will be found, by substituting representative values for the constants, that

- (i) B is always positive and large;
- (ii) C is small but positive and increases with z ;
- (iii) D is always very small, in practical cases. But we have already shown that the position of dynamic equilibrium, if it exists, is statically stable. Hence, since

$$D = - \frac{b}{\rho V^2 d^3} \frac{\partial M'}{\partial b} \quad (75)$$

we always have $D > 0$, provided $z < z^*$.

- (iv) Owing to the small value of D , $(BC - AD)$ is always positive: it increases with z .

Now consider the auxiliary equation.

$$A\lambda^3 + B\lambda^2 + C\lambda + D = 0 \quad (76)$$

Since B is large, while C and D are small, this equation always has one large negative root, approximately equal to $-B/A$. Hence we may divide out the corresponding factor and express (76) as

$$(A\lambda + B) \left(\lambda^2 + \frac{BC - AD}{B^2} \lambda + \frac{D}{B} \right) = 0 \quad (77)$$

The large negative root corresponds to a rapid subsidence with decay time (to $1/e$ th disturbance) equal to Ad/BV . The quadratic factor corresponds to a slow oscillation or a slow subsidence, according as the roots are complex or real.

Before developing this theory further, we consider an example. Take the case of an average Uncle Tom projectile for which

$$L = 10 \quad n = 3 \quad \sigma = 25 \quad \nu = 0.25 \quad z = 0.42 \quad b = 1.02 \quad L\beta = 0.36$$

$$\bar{\delta} = 0.20 \quad \bar{I\alpha} = 0.56 \quad f' = 0.47 \quad f = 0.162 \quad f_1'' = 0.0192 \quad f_2 = 0.00151$$

Then computation gives:

$$A = 3.08 \quad B = 27.5 \quad C = 1.82 \quad D = 0.0431 \quad EC - AD = 50.0$$

The stability conditions are all satisfied, and the auxiliary equation (77) becomes

$$(\lambda + 8.93) (\lambda^2 + 0.0660\lambda + 0.001565) = 0 \quad (78)$$

The decay time of the rapid subsidence is $0.11 d/V$; this is of a much lower order than the time taken (first) to attain the equilibrium value of δ : the subsidence is therefore so rapid that it can be ignored from the point of view of the external ballistics. The quadratic factor yields roots $(-0.0330 \pm i 0.0218)$, corresponding to a damped oscillation of period $288 d/V$. During this phase, taking typical values $V = 800$ ft./sec., $\delta_0 = 50$ sec⁻¹, we have

$$\varepsilon = \exp(-0.0330 \frac{Vt}{d}) \left[2.132 \sin(0.0218 \frac{Vt}{d}) - 0.2 \cos(0.0218 \frac{Vt}{d}) \right] \quad (79)$$

from which it can be shown that the projectile overshoots the equilibrium position when $Vt = 4.28 d$, and continues with $\delta > \bar{\delta}$ until it ceases to be of practical importance ($\varepsilon = 0.01$ say) when $Vt = 132 d$; the subsequent oscillations are negligible. In other cases, the quadratic factor leads to small negative real roots, corresponding to a combination of subsidences.

So, in general, within the limits we have set, the perturbation dynamics of the body are governed by the differential equation

$$\ddot{\varepsilon} + \frac{EC - AD}{B^2} \frac{V}{d} \dot{\varepsilon} + \frac{D}{B} \frac{V^2}{d^2} \varepsilon = 0 \quad (80)$$

or

$$\frac{d^2 \varepsilon}{ds^2} + \frac{EC - AD}{B^2} \frac{1}{d} \frac{d\varepsilon}{ds} + \frac{D}{B} \frac{1}{d^2} \varepsilon = 0 \quad (81)$$

where s is the arcual travel of the centre of gravity from its position at the instant of tail contact. In practice it is likely that the coefficient of the middle term will be greater than here indicated, owing to the viscous damping.

Two cases now arise, according to the nature of the roots of the auxiliary equation corresponding to (80) and (81).

Case I. Real roots $-r, -r'$

Here the motion is a combination of subsidences, governed by

$$\varepsilon = K \exp\left(-\frac{rVt}{d}\right) + K' \exp\left(-\frac{r'Vt}{d}\right) \quad (82)$$

where the constants K, K' are given by the initial conditions as

$$K = \frac{\bar{\delta}}{r - r'} \left(\dot{r}' - \frac{\dot{\delta}_0 d}{\delta V} \right) \quad K' = \frac{\bar{\delta}}{r - r'} \left(\frac{\dot{\delta}_0 d}{\delta V} - r \right) \quad (83)$$

For practical values of $\dot{\delta}_0 d / \delta V$, this always gives K, K' of opposite signs, the positive amplitude being associated with the smaller root r . Hence the motion is always a difference of subsidences; of such a type that the projectile overshoots equilibrium at an early stage, recovering aperiodically thereafter: this behaviour we shall, for brevity, describe as "semi-aperiodic". In any given case, the duration of the adjustment phase, i.e. the period during which the disturbance is of practical importance, can be deduced from (82): it is always of substantial length. Over such ranges, it is of course strictly not permissible to regard V as constant, as we have done. However, the indirect effect of velocity changes, by introducing acceleration components into (69) and (71) is a second-order complication of which account need not be taken in the present state of underwater ballistics: the direct effect can easily be allowed for by taking the differential equation in the form (81) with solution

$$s = K \exp\left(-\frac{rs}{d}\right) + K' \exp\left(-\frac{r's}{d}\right) \quad (84)$$

where

$$K = \frac{\bar{\delta}}{r - r'} \left(\dot{r}' - \frac{\dot{\delta}_0 d}{\delta V_0} \right) \quad K' = \frac{\bar{\delta}}{r - r'} \left(\frac{\dot{\delta}_0 d}{\delta V_0} - r' \right) \quad (85)$$

and V_0 is the speed of the centre of gravity at the instant of tail contact. This form avoids explicit mention of the variable velocity V , and, more conveniently, relates the disturbance to the independent variable s .

During the adjustment phase, we have

$$\begin{aligned} \dot{s} &= -\frac{V}{d} \left[rK \exp\left(-\frac{rs}{d}\right) + r'K' \exp\left(-\frac{r's}{d}\right) \right] \\ \ddot{s} &= \frac{V^2}{d^2} \left[r^2K \exp\left(-\frac{rs}{d}\right) + r'^2K' \exp\left(-\frac{r's}{d}\right) \right] \\ \text{obdu} &= \left[\frac{f_1}{d} r^2 - 2fr + \frac{f + L\bar{\alpha}f' + \frac{1}{2}V}{L} \right] K \exp\left(-\frac{rs}{d}\right) \\ &\quad + \left[\frac{f_1}{d} r'^2 - 2fr' + \frac{f + L\bar{\alpha}f' + \frac{1}{2}V}{L} \right] K' \exp\left(-\frac{r's}{d}\right) \end{aligned} \quad (86)$$

from which all necessary details follow. For example, it is possible to determine the maximum acceleration. On account of the exponential terms, (86) indicates maximum value at contact: this does not precisely represent the exact state of affairs, since at the instant of contact, deceleration due to tail forces is zero. The discrepancy is reconciled by the rapid subsidence which we have neglected. This however quickly decays so that we have the maximum, in practice, shortly after contact. Thus, apart from a very short-term deceleration, immediately after entry, the maximum value of $-\ddot{s}$ is approximately obtained by putting $t = 0$ in (86) as

$$\ddot{\epsilon}_{\max} = rr' \bar{\delta} \frac{V_0^2}{d^2} - (r + r') \frac{\dot{\delta}_0 V_0}{d} \quad (87)$$

This is additional to the "equilibrium" deceleration of the centre of gravity; so that

$$\text{max. transverse acceleration} = V^2 \bar{C} + (1-\bar{z}) \left[(r+r') \dot{\delta}_0 V_0 - rr' \frac{V_0^2}{d} \right] \quad (88)$$

it being understood that this gives a "long-term" value.

Again $\Delta \bar{\phi}$, the total (incremental) change of trajectory angle during the adjustment phase, can be obtained by integrating u between limits $s = 0$ to ∞ ; we find, after reduction,

$$\sigma b \Delta \bar{\phi} = 2f \bar{\delta} - \frac{f_1 \dot{\delta}_0 d}{\bar{\alpha} V_0} + \frac{f + L \bar{\alpha} f' + \frac{1}{2} v}{L} \left(\frac{K}{r} + \frac{K'}{r'} \right) \quad (89)$$

This is additional to the change ϕ on account of the "equilibrium trajectory".

Case II. Complex roots $(-k \pm ip)$

Here the motion is a slow, damped oscillation in accordance with

$$\epsilon = \exp \left(-\frac{kVt}{d} \right) \left[K \sin p \frac{Vt}{d} + K' \cos p \frac{Vt}{d} \right] \quad (90)$$

where

$$K = \frac{\bar{\delta}}{p} \left(\frac{\dot{\delta}_0}{\bar{\delta}} \frac{d}{V} - k \right) \quad K' = -\bar{\delta} \quad (91)$$

or, in the form independent of speed variation

$$\epsilon = \exp \left(-\frac{ks}{d} \right) \left[K \sin \frac{ps}{d} + K' \cos \frac{ps}{d} \right] \quad (92)$$

where

$$K = \frac{\bar{\delta}}{p} \left[\frac{\dot{\delta}_0 d}{\bar{\delta} V_0} - k \right] \quad K' = -\bar{\delta} \quad (93)$$

Also

$$\dot{\epsilon} = \frac{V}{d} \exp \left(-\frac{ks}{d} \right) \left[(pK - kK') \cos \frac{ps}{d} - (kK + pK') \sin \frac{ps}{d} \right] \quad (94)$$

After a distance given by

$$\cot \frac{ps}{d} = \frac{1}{p} \left(\frac{\dot{\delta}_0 d}{\bar{\delta} V_0} - k \right) \quad (95)$$

the tail overshoots equilibrium and then recovers in oscillations of wavelength $2\pi d/p$: the damping imposes a factor $\exp(-2\pi k/p)$ on the amplitude, per wavelength. It is easy to decide in any particular case whether the tail will leave the water on the second half-period.

The duration of the adjustment phase also follows from (92), e.g. in the example above the oscillation is effectively damped out before the end of the first half-period, i.e. is virtually semi-aperiodic.

During this time,

$$u = \left[2f - \frac{BC-AD}{B^2} \frac{f_1}{\bar{u}} \right] \frac{1}{\sigma b} \frac{d\varepsilon}{ds} + \left[\frac{f+L\bar{a}f'+\frac{1}{2}\nu}{L} - \frac{f_1}{\bar{u}} \frac{D}{E} \right] \frac{\varepsilon}{\sigma b d} \quad (96)$$

If necessary, this can be expressed in terms of z , by means of (92). The total incremental change of trajectory angle ($\Delta\bar{\phi}$) during the adjustment phase can be found by integrating u between limits $s = 0$ and ∞ :-

$$\sigma b \Delta\bar{\phi} = \left[2f - \frac{f+L\bar{a}f'+\frac{1}{2}\nu}{L} \frac{BC-AD}{BD} \right] \bar{\delta} - \left[\frac{f_1}{\bar{u}} - \frac{f+L\bar{a}f'+\frac{1}{2}\nu}{L} \frac{B}{D} \right] \frac{\dot{\delta}_0 d}{V_0} \quad (97)$$

In the example cited, this gives $\Delta\bar{\phi} = 3.25^\circ$, representing a major effect.

Also, by a similar argument to that used in Case I, the long-term

$$\text{max. transverse acceleration} = V_0^2 \ddot{c} + (1-z) \left[2k\dot{\delta}_0 V_0 - (k^2+p^2) \bar{\delta} \frac{V_0^2}{d} \right] \quad (98)$$

It is of interest to enquire how the oscillatory behaviour depends on centre of gravity position. For this purpose, we have again taken the class of projectile for which

$$L = 10 \quad n = 3 \quad \sigma = 25 \quad \nu = 0.25 \quad L\bar{a} = 0.36$$

and computed the values of the stability coefficients over a range of values of z . Fig. 12 shows the resulting values of damping constant $k = (BC-AD)/2B^2$ and frequency constant $p = (D/B-k^2)^{1/2}$. Two conclusions emerge:

- (i) The damping constant does not vary greatly with C.G. position.
- (ii) The frequency constant increases rapidly as the C.G. moves forward from the critical value: the wavelength diminishes correspondingly. With a very forward centre of gravity position, several periods may be completed before the oscillation is damped out*. By way of illustration, Fig. 13 shows the oscillations for the case $z = 0.35$, when $p = 0.1083$, $k = 0.0271$, and with $V_0 = 1,000$ ft./sec. and $\dot{\delta}_0 = 50$ sec.⁻¹. We therefore have the explanation of the pronounced oscillations which have been noticed experimentally (Ref. 6) in the case of models with forward C.G.'s. In the example given, the projectile almost loses contact with the cavity wall on the first rebound. If the value of $\dot{\delta}_0$ be higher, as in Ref. 6, the tail will execute oscillations in and out of the water. Such effects should be avoided in underwater weapon design since they imply periodicity in the curvature, and therefore loss of total lift.

5.3 Trajectories

Hitherto, the trajectories of long models projected at shallow angles (up to 20°) and high speed have been generally assumed to be capable of representation as

- (a) a (nearly) straight portion during which only the nose is wetted; and
- (b) a circular arc commencing at the position of tail contact, the

* The discovery of this effect is due to Butterworth.

curvature remaining constant until the gravitational effect predominates. The time of tail contact is given by Blackwell (Ref.3), who also deals with the conditions during phase (a) and gives a first-order treatment of phase (b), assuming dynamic equilibrium.

The analysis given above (5.1 and 5.2), however, shows that this simple picture is not adequate. The following phases may now be distinguished:-

- (a) a nearly straight portion; with this we have no concern in the present report (for details see Ref.3).
- (b) an adjustment phase commencing at the instant of tail contact and lasting for a substantial time, during which the projectile settles down to dynamic equilibrium. Typically, the tail overshoots the equilibrium position and recovers either in a slow subsidence or in a slow, damped oscillation. In the latter event the period is related to the distance of the centre of gravity forward of its critical position ($z^* - z$) so that, if the C.G. is very forward, a number of complete oscillations will occur, while if the C.G. is nearer its critical position, the oscillation will be damped out on the first half-period and the motion is virtually semi-aperiodic. The adjustment phase connotes rapidly varying curvature; it must be taken into account in an accurate description of trajectories, and in their tactical exploitation. The existence of this phase also stultifies experimental determinations of average curvature over the early part of the trajectory, if the end-point is arbitrary, and no doubt accounts in part for the observed scatter (Ref.4).
- (c) after a time which can be ascertained in any given case, the initial oscillation is damped down to insignificance and the projectile continues in dynamic equilibrium. During this time, it is likely that the velocity will have fallen so as to render consideration of gravity necessary; this is easily done. Eventually the curvature is reversed.

The foregoing description of the behaviour is well borne out by such experimental evidence as is available. Close verification must await the development of sequence arditron-photography.

We proceed to consider phase (c) first. Equation (48) can be written in the form

$$\bar{\sigma} = c_0 - \frac{F}{bv^2} = c_0 - \frac{F}{bv_0^2} \exp\left(\frac{2s}{h}\right) \quad (99)$$

where

$$c_0 = \frac{(\bar{\sigma} + L\beta)f(\bar{\sigma}) + \frac{1}{2}v(\bar{\sigma} + L\beta + LY)}{Ld(\sigma + \frac{1}{2}vLz)} \quad (100)$$

the curvature corresponding to zero gravity effect. The second term in (99) represents the gravity correction, and shows that gravity is, in effect, diluted in the ratio $1/b$. Then by integration of (99), the intrinsic equation of the trajectory (path of the C.G.) is

$$\phi = c_0 s - \frac{gh}{2bv_0^2} \left(\exp \frac{2s}{h} - 1 \right) \quad (101)$$

where the trajectory angle ϕ and arc s are measured from the position of the C.G. when the tail makes contact. From this equation, any "dynamic equilibrium" trajectory can be plotted. In practice, it is simpler, and sufficiently accurate, to plot by adjusting the circular trajectory for (diluted) gravity drop at each instant, the trajectory always having small inclination to the horizontal.

The increases of curvature \bar{c} on increasing v or z (with consequent increase of $\bar{\delta}$) can easily be demonstrated from (100): these effects are well-known in experiment (Ref.4).

Now consider phase (b), which we have studied as a perturbation of dynamic equilibrium (5.2). The added curvature u is given by (69), and total lift coefficient varies proportionally. By successive integration, the added trajectory angle $\Delta\phi$ and added ordinate Δy are found as

$$\left. \begin{aligned} \Delta\phi &= P \left(\frac{d\varepsilon}{ds} - \frac{\dot{\delta}_0}{V_0} \right) + Q \frac{1}{d} (\varepsilon + \bar{\delta}) \\ \Delta y &= P \left(\varepsilon + \bar{\delta} - \frac{\dot{\delta}_0 s}{V_0} \right) + Q \left[\frac{\bar{\delta} s}{d} - \frac{Bd}{D} \left(\frac{d\varepsilon}{ds} - \frac{\dot{\delta}_0}{V_0} \right) - \frac{BC-AD}{ED} (\varepsilon + \bar{\delta}) \right] \end{aligned} \right\} (102)$$

where

$$P = \left[\frac{f_1}{\alpha} - \frac{f + L\bar{\alpha}f' + \frac{1}{2}v}{L} \cdot \frac{B}{D} \right] \frac{d}{cb} \quad Q = \left[2f - \frac{f + L\bar{\alpha}f' + \frac{1}{2}v}{L} \frac{BC-AD}{ED} \right] \frac{d}{cb} \quad (103)$$

Hence $\Delta\phi$ and Δy can be evaluated for any point in the adjustment phase and applied as a correction to the equilibrium trajectory. This correction is substantial: after the oscillation has disappeared, the trajectory has been rotated ($\Delta\bar{\phi}$) and lifted ($\Delta\bar{y}$), where

$$\left. \begin{aligned} \Delta\bar{\phi} &= -P \frac{\dot{\delta}_0}{V_0} + Q \frac{\bar{\delta}}{d} \\ \Delta\bar{y} &= P \left(\bar{\delta} - \frac{\dot{\delta}_0 \bar{s}}{V_0} \right) + Q \left(\frac{\bar{\delta} \bar{s}}{d} + \frac{Bd}{D} \frac{\dot{\delta}_0}{V_0} - \frac{BC-AD}{ED} \bar{\delta} \right) \end{aligned} \right\} (104)$$

in which \bar{s} denotes the total travel at this point. These two effects combine to increase the effective path of the projectile. The proper exploitation of this phase is therefore important in the design of underwater projectiles.

By way of illustration, we take up again the numerical example considered in (5.2). For this case, $e_{0z} = 1/1230 \text{ ft.}^{-1}$; and assuming $V_0 = 800 \text{ ft./sec.}$ and $h = 300 \text{ ft.}$, \bar{c} is as shown in Fig. 14; the fall-off is due to gravity. This figure also shows the actual curvature ($\bar{c} + u$) developed during the adjustment phase: It attains a maximum value about $2\frac{1}{2}$ times that of \bar{c} ; the average value is also considerably higher. Due to this cause, there is a total rotation of the trajectory $\Delta\bar{\phi} = 3.25^\circ$ during the adjustment phase. Fig. 15 shows two trajectories corresponding to $\phi = -12^\circ$ at the origin (position of centre of gravity at the instant of tail contact):-

- (a) the trajectory as it would be if the equilibrium dig-ratio were maintained throughout;

- (b) the actual trajectory, allowing for the adjustment effects.

The inadequacy of dynamic equilibrium as a complete representation of the motion is apparent.

We have now to consider how all this bears on the design of weapons for underwater attack. Take first the considerations in so far as they are revealed by the concept of dynamic equilibrium. Then the design problem is the provision of adequate equilibrium lift, for the minimum total drag. To minimise drag with a lift-producing head, the obvious and hallowed expedient is to place the head on a base of reduced diameter, so that the frontal area of the wetted nose is cut down as much as possible, without wetting the shoulder of the projectile. Then, for a head of given shape, drag is reduced proportionally to the square of the decreased diameter. However, ν is reduced in similar ratio. To maintain the same lift, (46) shows that $\bar{\alpha}$ must be increased and the projectile travels at increased equilibrium yaw. Simultaneously $\bar{\sigma}$ is increased, so that there is risk of instability: this is a well-known experimental effect. The practical means of securing the same lift are:-

- (a) moving back the centre of gravity in accordance with (53);
- (b) seeking a basic head shape for which ν is higher: from (43), it would seem that sharp cones are the most efficient, in this respect.

Thus the forcing of the minimum drag requirement to extremes is bound to lead to the C.G. entering the sub-critical zone. In this condition, as we have seen, $\bar{\sigma}$ is virtually indeterminate, a random element enters, and dispersion is the result. Up to a point, this is acceptable: the decision as to how far we may trespass on the sub-critical zone rests, in any given case, on a statistical calculation of efficiency in terms of drag, lift and dispersion (see Ref.7); but such figures may alter in the transition from model to full scale.

The foregoing considerations, strictly, apply only to phase (c). The analysis of (5.1) and (5.2), however, indicates that design should also make the best use of the adjustment phase. Assuming given overall lift qualities, the best type of trajectory is one in which the projectile is held at lethal depth for the maximum possible distance. To achieve this, the distribution of curvature should be such that a high level is maintained at an early stage, to secure rotation of the trajectory to a nearly horizontal path, followed by a moderate value approximately sufficient just to offset gravity: this is the ideal "skimming trajectory". The method of achieving this would be to induce a "semi-aperiodic" adjustment phase leading to the appropriate values of $\Delta\bar{p}$ and $\Delta\bar{y}$. This we have seen is largely a matter of centre of gravity position: for any given shape, the C.G., for semi-aperiodic vibration, is restricted to a quite narrow zone forward of the lower critical position (because of rapid increase of p). Where z is restricted by structural considerations to low values, of the order of 0.3 and less, the ideal is more difficult to attain: in such cases, the ideal trajectory can only be obtained by moving the critical position forward: means of achieving this are discussed in (6.1). For favourable oscillatory characteristics, there is an upper limit to $(z^* - z)$: this can be determined in any given case from a p, k graph of the type exemplified in Fig.12.

To recapitulate, the forward limit to the centre of gravity

position is set by the necessity of avoiding any appreciable rebound above the equilibrium position. The rearward limit is at the point where increasing dispersion commences to outweigh the advantage of increased lift. In practice, the location of these points would be deduced from model experiment rather than theory. However it should be expected that these limits would alter on passing to full scale, since closed cavities do not, in general, scale up according to the Froude law. The theoretical formulae might enable the scale effects to be forecast, when the necessary cavity data are available.

5.4 Rotated projectiles

The underwater behaviour of axially spun projectiles is a problem of growing importance because of its applicability to both shell and spinning rockets. Since, however, experimental study of this aspect of underwater ballistics is still in its infancy, a detailed treatment, such as that given above for unrotated projectiles, would be out of place at present. The discussion which follows is intended merely to deal briefly and simply with fundamentals. When some practical data are available, it will be desirable to extend this theory further.

The problem can be treated by the ordinary method of gyro dynamics, together with the principles laid down in the earlier part of this Note. Apart from the viscous couple damping the rotation, the force system may, in a first-order treatment, be assumed to be the same as that detailed in (5.1) for a non-rotated projectile. (Some experiments carried out in the Admiralty water-tunnel at Haslar indicated that the shape of the cavity is not affected by the spin). The nose and tail forces combine to create a moment about a transverse axis through the centre of gravity: this results in precession, so that the tail circulates round the cavity wall. We shall consider only steady precession (i.e. no nutation), not because this type of motion necessarily occurs, but because it is physically evident that, as with a nearly vertical top, the possibility of such a mode of motion implies stability in the actual oscillations which occur, and vice versa. The associated motion of the C.G. is helical.

In steady precession, in spite of motion of the cavity relative to the centre of gravity, the dig-ratio remains constant (= $\bar{\delta}$, say): this results in considerable simplification of the equations of motion. Likewise $\bar{\alpha}$ retains the small constant value $\bar{\alpha}$, and

$$L\bar{\alpha} = \bar{\delta} + L\beta \quad (105)$$

where L and β have the same significance as in (5.1). Then, as in (5.1),

$$\left. \begin{aligned} L_T &= \rho V^2 d^2 \bar{\alpha} f(\bar{\delta}) \\ M_T &= \frac{16}{15} \rho V^2 d^3 f_1(\bar{\delta}) \\ M_T^* &= \frac{16}{15} \rho V^2 d^3 [f_1(\bar{\delta}) - L\bar{\alpha}(1-z)f(\bar{\delta})] \end{aligned} \right\} \quad (106)$$

Also

$$M_N^* = \rho V^2 d^3 \mu(\bar{\alpha} + \gamma) \quad (107)$$

where μ is a constant, and the small effects on the nose incidence due to the curvature and torsion of the trajectory have been neglected. For lift-producing heads,

$$\mu = \frac{1}{2} \nu Lz \quad (108)$$

agreeing with (46): but (107) also includes no-lift (and small lift) heads for which μ is approximately independent of z , and usually negative. It is urgently necessary that some practical determinations of μ , for such types of head, be made.

Hence the total moment about the centre of gravity is given by

$$M' = \rho V^2 d^3 J \quad (109)$$

where

$$\left. \begin{aligned} J &= \mu(\bar{\alpha} + \gamma) && \text{when } \alpha < \beta \\ &= \mu(\bar{\alpha} + \gamma) + \frac{16}{15} [f_1(\bar{\delta}) - L\bar{\alpha}(1-z)f(\bar{\delta})] && \text{when } \alpha > \beta \end{aligned} \right\} (110)$$

If ω be the angular velocity about the longitudinal axis of the body, A the moment of inertia about a transverse axis through the C.G., and C the moment of inertia about the longitudinal axis of symmetry, then Ω , the precessional angular velocity, is given by

$$A\Omega^2 - C\omega\Omega + \rho V^2 d^3 \frac{J}{\alpha} = 0 \quad (111)$$

For the precession to exist, i.e. for the roots of this equation to be real, the condition is

$$C^2 \omega^2 \bar{\alpha} > 4A\rho V^2 d^3 J. \quad (112)$$

which reduces to

$$\left. \begin{aligned} 0 &> \frac{15}{16} \left[\mu(\bar{\alpha} + \gamma) - \frac{C^2 \omega^2 \bar{\alpha}}{4A\rho V^2 d^3} \right] \\ \text{or} \quad L\bar{\alpha}(1-z)f(\bar{\delta}) - f_1(\bar{\delta}) &> \frac{15}{16} \left[\mu(\bar{\alpha} + \gamma) - \frac{C^2 \omega^2 \bar{\alpha}}{4A\rho V^2 d^3} \right] \end{aligned} \right\} (113)$$

according as $\alpha \leq \beta$. If μ is negative, this condition can always be satisfied either with the tail in contact or not. If μ is positive (lift-producing heads), we may write the second (and more lax) condition as

$$L\bar{\alpha}(1-z)f(\bar{\delta}) - f_1(\bar{\delta}) > \frac{15}{32} \left[\nu Lz (\bar{\alpha} + \gamma) - \frac{C^2 \omega^2 \bar{\alpha}}{2A\rho V^2 d^3} \right] \quad (114)$$

In this expression, the term involving ω is, for practical values of the constants, a small one. Hence the effect of spin, although it does assist in the maintenance of stability, is very slight. Physically, this corresponds to the fact that the body now finds itself in a medium about 800 times as dense as air. The spin effect would be made appreciable if shell could be spun at 20 or 30 times the prevalent angular rates, but this is not a practical possibility. For rotating rockets, where the spin is usually very

low, the stabilising effect is quite negligible.

Now, for a given value of $\bar{\delta}$, the left-hand side of (114) decreases with increasing z , while the right-hand side increases. Thus, as the centre of gravity is moved backwards, the inequality becomes more difficult to satisfy, until when

$$L\bar{\alpha}(1-z)f(\bar{\delta}) - f_1(\bar{\delta}) = \frac{15}{32} \left[\nu Lz(\bar{\alpha} + \gamma) - \frac{C^2 \omega^2 \bar{\alpha}}{2A\rho V^2 d^3} \right] \quad (115)$$

we have the limiting case in which precession is only just possible: then (111) has equal roots and

$$\Omega = \frac{C\omega}{2A} \quad (116)$$

corresponding to a precessional rate much slower than the spin. Further, if we neglect the very small spin term in (115), we recover equation (53), governing the dynamic equilibrium of the unrotated projectile: the properties of this relation and the existence of a critical value of z have been discussed in (5.1). We therefore reach the following general principle:-

Subject to a slight marginal effect on account of spin, a cavitating projectile will be stable under rotation, if it is stable under the same conditions without rotation, and vice versa.

For shell, this condition is a very onerous one. The comparatively rearward C.G.'s necessitated by structural considerations can be counteracted in air by provision of spin. This is of no avail in water, where also, owing to the short length, stability cannot be obtained from the tail forces. For example, consider a conventional (1.4 c.r.h.) shell for which

$$L = 5 \quad \nu = 0.37 \quad L\beta = 0.25 \quad L\gamma = 0.08$$

Then calculation from (115), neglecting the spin term, gives the following table:

$\bar{\delta}$	0	0.1	0.2	0.3	0.4	0.5	0.6	0.7	0.8	0.9	1.0
lim z	0	0.279	0.325	0.336	0.335	0.341	0.342	0.343	0.344	0.345	0.347

Centre of gravity positions of this order are impracticable in shell design. Hence the impossibility, observed in experiment, of stabilising conventional shell shapes under water. It follows that with neither spin nor tail forces available as a source of stabilization, types of head must be employed which provide a restoring moment, or, less stringently, for which μ , if positive, does not greatly increase with z . Fortunately, the requirements arising from the satisfactory entry of shell into water, at the shallow angles demanded, point in the same direction. The condition which μ must satisfy follows from (112), if the effect of spin be discounted, as

$$\mu < \frac{16}{15(\bar{\alpha} + \gamma)} \left[L\bar{\alpha}(1-z)f(\bar{\delta}) - f_1(\bar{\delta}) \right] \quad (117)$$

This implies loss of lift, but, owing to the helical nature of the

trajectory, lift is applied in all transverse directions and is of no great advantage in any event.

Thus rotated projectiles fall into two main classes, from the point of view of underwater ballistics:-

- (a) Rocket type: L is high enough to secure stabilization by the tail forces. The stability considerations are effectively those of the unrotated projectile, as described in (5.1) and (5.2). Here, owing to the precession, the lift is developed in part laterally, with consequent loss of efficiency, unless the spin be sufficiently reduced. Equation (116), interpreted roughly as the mean rate of precession, permits an estimate of the loss of efficiency in any given case.
- (b) Shell type: stability is obtained from a flat or nearly flat head. The path is a narrow helix, the axis of which has no upward curvature. The diameter of the head may be, up to a point, reduced, so as to diminish drag and obtain the maximum length of efficient underwater trajectory. If μ is negative, the round is then stable even without tail contact. If μ is positive (but small), stability can be achieved for the most rearward centre of gravity positions, at light draught. For example, taking a case for which

$$L = 5$$

$$L\beta = 0.25$$

and μ having such a value that the right-hand side of (109 b) is negligible, we obtain:

$\bar{\delta}$	0	0.1	0.2	0.3	0.4	0.5	0.6	0.7	0.8	0.9	1.0
lim z	1.000	0.859	0.738	0.664	0.612	0.583	0.558	0.539	0.526	0.513	0.504

There is also the class of projectile which receives accidental spin, e.g. smooth-bore models fired experimentally. There will be a very slow rate of precession, which may possibly account for lateral deviations, accompanied by loss of lift, observed in experiment.

The treatment we have given here for the rotated projectile is, as explained above, not intended to be complete. In particular, no account has been taken of the lift forces due to rotation (Magnus type forces). But the need at the moment is for further experimental rather than theoretical investigation.

6. Miscellaneous effects

6.1 Effect of tail shape

The need for obtaining optimum lift and oscillatory characteristics in an underwater projectile raises the question as to whether performance can be improved by judicious shaping of the tail. (By this term we refer to the rear of that part of the projectile which travels underwater). Such action might be directed towards:

- (a) improvement of the dynamic equilibrium trajectory, i.e. providing an increased lift not conveniently attainable by modifying the nose shape;
- (b) improvement of the adjustment phase where this would otherwise be insufficiently favourable.

Tail shaping acts in two ways:-

- (a) it alters the value of β , i.e. the angle of yaw at which tail contact is first made; e.g. tapering the tail increases β ;
- (b) for $\alpha > \beta$, it provides an increased or diminished moment M_T , according to the shape employed.

The method given in (2.3) for the unmodified cylinder can clearly be applied under the more general circumstances, allowing for variable d and α , and taking the value of $f(\delta)$ as defined in (3.1). For any given shape, the determination of lift and moment involves only computational difficulties: (Table I gives the necessary functions). For this reason no detailed examination is undertaken here, but we rest content with certain general observations.

Consider first the case where a protuberance is added to the tail of the uniform cylinder, e.g. the inclined circumferential flange on the tail of the German BT.1400. This has the effect of (a) reducing β , so that lift is developed sooner, and (b) increasing the lift at any given value of α (because of increased diameter of the relevant sections). Hence in (52) there is an increase of tail effect relative to nose effect, and equilibrium will be achieved at a smaller value of \bar{x} . This leads to smaller values of nose lift and of the balancing tail force, i.e. to an overall loss of lift. Here may possibly be the explanation of the deterioration of performance believed to be associated with retention of portions of tail assemblies on underwater rockets. Further, referring to (53), the replacement of $(\bar{x} + L\beta)f(\delta)$, by some function of greater value, means that, for any value of δ , the value of z_{∞} is increased. An increase in the critical value of z therefore occurs, and hence stability is possible for more rearward C.G. positions: this is, fundamentally, why the tail flange was found to stabilize the B.T. 1400.

Conversely, if the tail be reduced by shaping it to a contour within that of the uniform cylinder, without altering overall length, tail contact is delayed, \bar{x} is increased, and a greater total lift is developed. But this is achieved at the expense of reducing z^* . Thus it has been confirmed experimentally that Uncle Tom models which are just stable with a cylindrical tail become unstable when the tail is tapered slightly. However, in the case of projectiles with a very forward C.G. position (e.g. the L.A.P./R.P.), this risk does not arise, and a very considerable increase in lift should be obtainable by tapering or otherwise reducing the tail. The amount of reduction necessary is slight.

The above discussion relates to dynamic equilibrium: but we have also to consider the effects on the adjustment phase. The oscillatory behaviour is considerably influenced by the consequent movement of critical C.G. position. Thus tail increase, if the centre of gravity is unchanged, increases the natural frequency. Conversely, tail reduction, if stability is still maintained, tends to reduce the natural frequency: this may be a great advantage in the case of a projectile with very forward C.G. position, since the adjustment oscillation may be converted from the periodic to semi-periodic type.

Similar considerations apply to rotated projectiles. For very slowly spun rockets, the considerations are practically the same as those outlined above for unrotated rounds. For shell, which,

as we have seen, should be designed as no-lift shapes, there is no advantage, from the point of view of underwater ballistics, in reducing the tail: if this is done for air-ballistic reasons, the effect on underwater performance will in fact be unfavourable.

6.2 Residual problems

Among the most important of the problems left unresolved by the present Note is the effect of the transverse curvature of the cavity on the system of tail forces. Since the ratio of cavity diameter to projectile diameter in practical cases is of the order of 2 or 3, it is likely that this effect is an appreciable one. Preliminary study of this question has shown that accurate theoretical treatment would require a lengthy analysis out of place in the present context. It is recommended instead that the effect be measured by appropriate experimental investigation. This could easily be undertaken in a cavitation tunnel, which must in any event be employed to determine experimentally more accurate values of the virtual mass function $f(\delta)$, valid for the spray conditions of cavitating motion, to replace those of Table I based on towing tank measurements. Indeed, it is one of the major aims of this Note to urge that a quantitative knowledge of underwater behaviour can be attained only through comprehensive cavitation tunnel experiment, and that such work must be pursued if underwater projectiles are to be confidently designed.

It is perhaps worth mentioning that the apparent dig-ratio in arditron photographs exceeds the true value (Fig. 9) and that, in photo-analysis, allowance should also be made for the optical distortion caused by the cavity acting as a cylindrical air-lens.

The longitudinal curvature of the cavity at the position of tail contact is, in comparison, small (see Fig. 9), and allowance for this effect would be merely a refinement.

Another problem to which we have paid no attention is the effect of the tail-loading on the (non-rigid) projectile. This has two aspects:-

- (a) flexure of the body, as a loaded tube, with resultant effects on tail incidence, critical C.G. position, etc:
- (b) strength requirements in the projectile body.

Both these matters are easily dealt with, since the distribution of tail load is now known from (11). It is understood that the first of these is under investigation at G.F.R.S.: the second lies outside the scope of the present paper.

7 Conclusions

It has been shown that the lift forces arising on a planing cylinder, as measured by towing tank experiment, can be adequately accounted for by a theory of the virtual mass type, taken together with a spray effect. By means of certain theoretical assumptions, it is possible to discover the lift distribution over the wetted area, and thus to obtain generalised lift and moment results for modes of motion other than planing, and for tail shapes other than circular cylinders.

With the aid of a simple representation of nose forces, it has therefore been possible to specify the force system on a long cavitating projectile with some completeness. Deducing from this

the type of steady motion known as "dynamic equilibrium" we have been able to discover how the tail immersion affects the motion, and also to demonstrate the importance of centre of gravity position. The existence of a critical point is established theoretically, and found to agree closely with experimental values. It is also shown that there is a sub-critical zone of C.G. positions; if the centre of gravity encroaches too closely on this zone, a degree of dispersion results.

The quantitative as well as the qualitative agreement of the results with experiment indicates that the fundamental theoretical assumptions are reliable.

Further, the complete force system enables the dynamic characteristics of the projectile to be studied. It is shown that the longitudinal oscillations are governed by a differential equation of the second order; formulae are given which enable the effects of the initial oscillation after tail-contact to be calculated for every point until it is damped out. This "adjustment phase" has a substantial effect on the trajectory, and means are considered whereby it can be exploited to give the ideal of high lift in the early stages, and low lift later. Briefly, this consists of lessening the distance between centre of gravity and the critical point (by movement of either) and thereby increasing the half-wave-length of the initial overshoot until this occupies virtually the whole of the damping distance.

The differential equation also enables maximum tail decelerations to be evaluated.

For rotated projectiles also, it is possible to demonstrate the fundamental properties on the basis of the prescribed tail force system. A static condition analogous to dynamic equilibrium exists, provided the centre of gravity is forward of a critical position: this critical position is practically the same as for the same projectile unrotated. Spin has only a very small stabilizing effect, so that stability can be achieved only by

- (a) sufficient length for tail stabilization (rocket type); or
- (b) nearly flat head for nose stabilization (shell type).

In the first case, the considerations are virtually the same as for the unrotated projectile. In the second case, one is committed to a virtually linear underwater path. The oscillatory (nutatory) characteristics of rotated projectiles could be investigated along similar lines, but this work is deferred until more experimental data are available.

Theory should not proceed too far without parallel experiment. In the present case, towing-tank measurements have been taken as a basis. The conditions are not strictly comparable, owing to the effects of spray and absence of curvature in the water surface; they were used because they were the only experimental data extant. An effort has been made to eliminate or reduce the spray effect, and the agreement obtained on lifts and critical C.G. positions with those found experimentally in the G.F.R.S. tanks, indicates that this may have been done successfully. Nevertheless, it is urgently necessary that investigation be made in the more nearly comparable conditions prevailing in a cavitation tunnel. Such experiment should be directed in the first instance to amassing comprehensive data on (separate) nose and tail forces and moments, for a range of geometrical shapes. The effect of transverse cavity curvature should be covered

incidentally. Secondly a firm experimental basis should be provided for the study of oscillatory characteristics by investigation of the moment-rotary derivatives associated with pitching. If possible, provision should be made for similar study of the complete force system on rotated projectiles. Research into cavity forms, both theoretical and experimental, should proceed at the same time. Finally, the role of tank firings would be to confirm the completely specified force system, and to decide the effects of underwater deceleration not conveniently reproducible in the cavitation tunnel.

It is anticipated that such experiment would confirm the fundamental formulae employed in the present paper, but with rather different values for the virtual mass and associated functions from those in Table I. With these more reliable values, it would be worth while to make the various extensions of the theory which have been indicated above.

The implications of the present paper for design are not easily summed up in a few words. It is not possible to provide the designer of an underwater projectile with precise requirements, or with comprehensive and codified data. The optimum placing of the centre of gravity, especially, involves fine considerations, and is therefore vulnerable to scale effects. Nevertheless, a few generalisations may safely be made which will supplement the designer's background of underwater ballistics, and perhaps rationalize the apparently arbitrary demands sometimes made upon him:-

- (a) Unrotated projectiles: the total lift, for a given shape and weight, increases with backward movement of the C.G., until, at a certain point, instability results. Below this critical point is a small sub-critical zone in which the projectile attains nearly neutral stability, resulting in dispersion. The conception which has been used hitherto, of a projectile riding at nearly constant yaw and in a path of constant curvature, is not adequate: there is an "adjustment phase" resulting from the initial oscillation, lasting for a substantial fraction of the effective underwater path, and having an important influence on the efficiency of the trajectory: the character of this phase depends on the distance of the centre of gravity forward of the critical point. The phase should be exploited, by suitable design, in order to give a "skimming trajectory".
- (b) Slowly rotated projectiles: the stabilizing effect of spin, below water, is negligible. Hence the stability criteria are the same as for unrotated projectiles. The spin, however, results in precession around the cavity wall, and unless this is sufficiently reduced, the effect of lift will be nullified or reduced.
- (c) Shell: the stabilizing effect of spin is again very small, and since the centre of gravity position and length/diameter ratio are normally such as to render tail stabilization impossible, a flat or nearly flat head must be employed. Precession is so rapid that any lift developed would be nullified in any event.
- (d) Tail-shaping: this artifice would have a material effect on underwater performance. In general, increase of the tail section results in loss of lift, but increased stability. Conversely, reduction of the tail section results in increased

SECRET

Tech. Note No. Arm. 344.

lift, but the stability is compromised: it also has the effect of increasing the wavelength of the initial oscillation. Tail-tapering may therefore be recommended for projectiles with very forward C.G. positions, which otherwise are liable to suffer from insufficient lift and too rapid oscillation in the adjustment phase.

- (e) Tail-bending: formulae are given which enable the flexure of the tail to be calculated, and also provide the basis for standard calculations of maximum stress and bending moment.
-

References

<u>No.</u>	<u>Author</u>	<u>Title, etc.</u>
1	H. Hogg and A.G. Smith	Forces on a Long Cylinder Planing on Water. R.A.E. Report No. Aero.1999. December, 1944.
2	E.G. Richardson	Impact on Water: a Summary. M.A.E.E. Report No. H/Arm./Res. 24 = U.B.R.C.30.
3	B.D. Blackwell	A Method of Prediction of the Upturning Underwater Trajectories of Rockets in Two Dimensions. Admiralty Report No. S.R.E./U.T./8. January, 1945.
4	R.A. Shaw and P.E. Naylor	Underwater Performance of 1 inch Diameter Models of a Family of Cone Head Rockets. M.A.E.E. Report No. H/Arm./Res. 25. February, 1945.
5	R.W. Duncan and F.E. Bradley	An Experimental Basis for the Development of a Method of Calibration of the Underwater Ballistic Properties of Projectile Forms. R.A.E. Technical Note No. Arm. 328. July, 1945.
6	S. Butterworth	Calculation of the Underwater Trajectory of a Projectile. Admiralty Report No. A.R.L./N.2/86-44/H = U.B.R.C. 37. April, 1945.
7	N. Simmons	Finnart Trials of 1/3 Scale Uncle Tom. M.A.E.E. Report No. H/Arm./Res. 26. March, 1945.

Attached:- Tables I and II.
 Sk. Nos. Arm. 21502 to 21510 inclusive.

Distribution:-

D.G.Arm.	Sec. O.B.
D.G.S.R.	D.G.P.
C.N.R.	D.P.D.
D.Arm.R.D.	C.S.P.D.E.
D.D.Arm.R.	C.E.A.D. (3)
N.A./D.Arm.R.D.	C.S.A.R.
R.D.Arm. 4.	D. of S., Adv. Arm. Course
R.D.Arm. 5.	D.S.R. Admiralty
R.D.Arm. 10.	A.R.L.
R.D.Arm. 14 (30)	D.N.C.
R.T.P./T.I.B. (45 + 1)	A. & A.E.E.
O.R.S. Coastal Command	T.D.U.
D.R.A.E.	Head of Cont. Weapons Dept.
G.S.(E).	G.F.R.S. (2)
Head of Arm. Dept.	Section 1.

Table I
Virtual mass and associated functions.

x	f'(x)	f(x)	f ₁ (x)	f ₂ (x)	f ₃ (x)	f ₄ (x)	f ₅ (x)	f ₆ (x)	f ₁ /f
0	1.232	0	0	0	0	0	0	0	0
0.1	0.792	0.105	0.0056	0.0003	0	0	0	0	0.053
0.2	0.464	0.162	0.0192	0.0015	0.0001	0	0	0	0.118
0.3	0.370	0.203	0.0375	0.0043	0.0004	0	0	0	0.185
0.4	0.332	0.236	0.0595	0.0091	0.0010	0.0001	0	0	0.252
0.5	0.310	0.271	0.0848	0.0162	0.0023	0.0003	0	0	0.313
0.6	0.295	0.301	0.1134	0.0260	0.0044	0.0006	0.0001	0	0.376
0.7	0.288	0.330	0.1449	0.0390	0.0076	0.0012	0.0002	0	0.438
0.8	0.288	0.358	0.1793	0.0551	0.0123	0.0022	0.0003	0	0.499
0.9	0.288	0.386	0.2165	0.0718	0.0188	0.0037	0.0006	0.0001	0.560
1.0	0.288	0.413	0.2565	0.0984	0.0275	0.0060	0.0011	0.0002	0.620

These functions are defined in (2.3) and (3.1). The values are based on towing tank measurements; ultimately more reliable values should be obtainable from cavitation tunnel experiment.

The following general results assist in computation when functions are expanded in series of powers of the horizontal distance x from the trailing edge.

$$\int_0^{\delta \cot \alpha} f'(\delta - \frac{x}{d} \tan \alpha) x^n dx = \frac{n}{n+1} (d \cot \alpha)^{n+1} f_n(\delta)$$

$$\int_0^{\delta \cot \alpha} f(\delta - \frac{x}{d} \tan \alpha) x^n dx = \frac{n}{n+1} (d \cot \alpha)^{n+1} f_{n+1}(\delta)$$

Table IIList of Symbols.

Virtual mass theory:

d	(horizontal) diameter of cylinder.
M	mass of cylinder (or mass per unit length).
ρ	density of water.
t	time, measured from first contact.
v	downward velocity of cylinder.
v_0	value of v at tail contact.
m	added mass (per unit length of cylinder).
z	submergence/diameter.
ℓ	lift force (per unit length of cylinder).
$f', f, f_1, f_2, f_3, f_4, f_5, f_6$	virtual mass functions (see Table I).
g	gravitational acceleration.
L	length/diameter ratio (measured from nose C.P.).
σ	specific gravity coefficient ($= \frac{M}{\rho d^3}$).
U	downward velocity of trailing edge.
V	forward velocity of trailing edge.
Ω	angular velocity of cylinder, in pitching plane.
α	angle of tail-incidence (radians).
δ	dig-ratio (trailing-edge submergence/diameter).
L_T	tail lift force (normal to direction of motion).
D_T	tail drag force (direction of motion reversed).
M_T	tail moment about trailing edge.
M_T^c	tail moment about centre of gravity.

Unrotated projectile:

β	value of α at which tail contact is first made.
γ	inclination of cavity surface to axis of cavity.
i	angle of incidence at the nose.
v	constant of proportionality for the nose lift.
L_N	nose lift force (normal to axis of projectile).
M_N	nose moment about the centre of gravity.
M^c	total pitching moment about the centre of gravity.
z	centre of gravity ratio (measured from nose C.P.).
z_{∞}	a first approximation to z.

(cont.)

- ω upward curvature of the trajectory.
 $\bar{\delta}, \bar{\alpha}, \bar{c}$ equilibrium values of δ, α, c respectively.
 z^* critical centre of gravity ratio.
 z_{∞}^* a first approximation to z^* .
 h travel parameter in retarded motion.
 n transverse radius of gyration about C.G./diameter.
 s arcular travel of C.G. }
 x forward travel of C.G. } measured from position
 y upward travel of C.G. } of C.G. at tail-contact.
 V_0 forward speed when $s = 0$.
 δ_0 value of δ when $s = 0$.
 G gravity correction. (see 49).
 H, H' retardation corrections (see 60).
 c_0 curvature in the absence of gravity drop.
 ϵ perturbation increment to $\bar{\delta}$.
 u perturbation increment to \bar{c} .
 $b = 1 + \frac{u_L z}{2\sigma}$.
 ϕ trajectory angle (in dynamic equilibrium).
 $\Delta\phi$ perturbation increment to ϕ .
 $\bar{s}, \Delta\bar{\phi}, \Delta\bar{y}$ values of $s, \Delta\phi, \Delta y$ on attainment of equilibrium.
 Λ, B, C, D stability coefficients.
 χ auxiliary stability variable.
 k damping constant.
 p frequency constant.

Rotated projectile:

- μ constant of proportionality for nose lift.
 ω angular velocity of projectile about longitudinal axis.
 Q precessional rate.
 A moment of inertia about transverse axis through the C.G.
 C moment of inertia about longitudinal axis of symmetry.

The above are assumed to be expressed in any self-consistent system of units. Cases where the notation overlaps will be clear from the context. Symbols used only transitorily have been omitted.

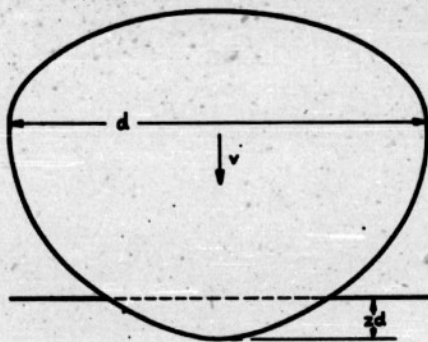


FIG. 1 IMMERSION OF A GENERAL CYLINDER.

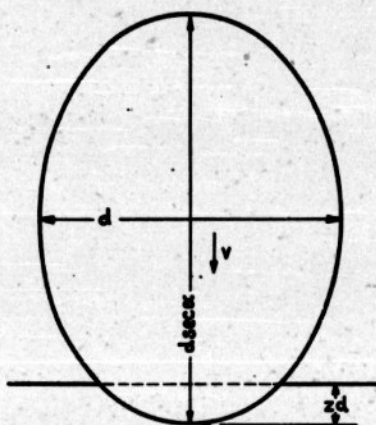


FIG. 2 IMMERSION OF AN ELLIPTIC CYLINDER.

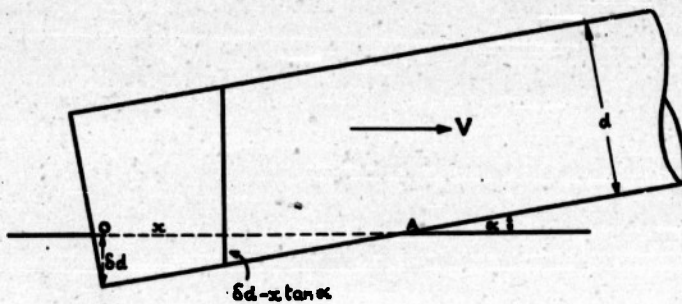


FIG. 3 THE PLANING CYLINDER.

FIG. 4.

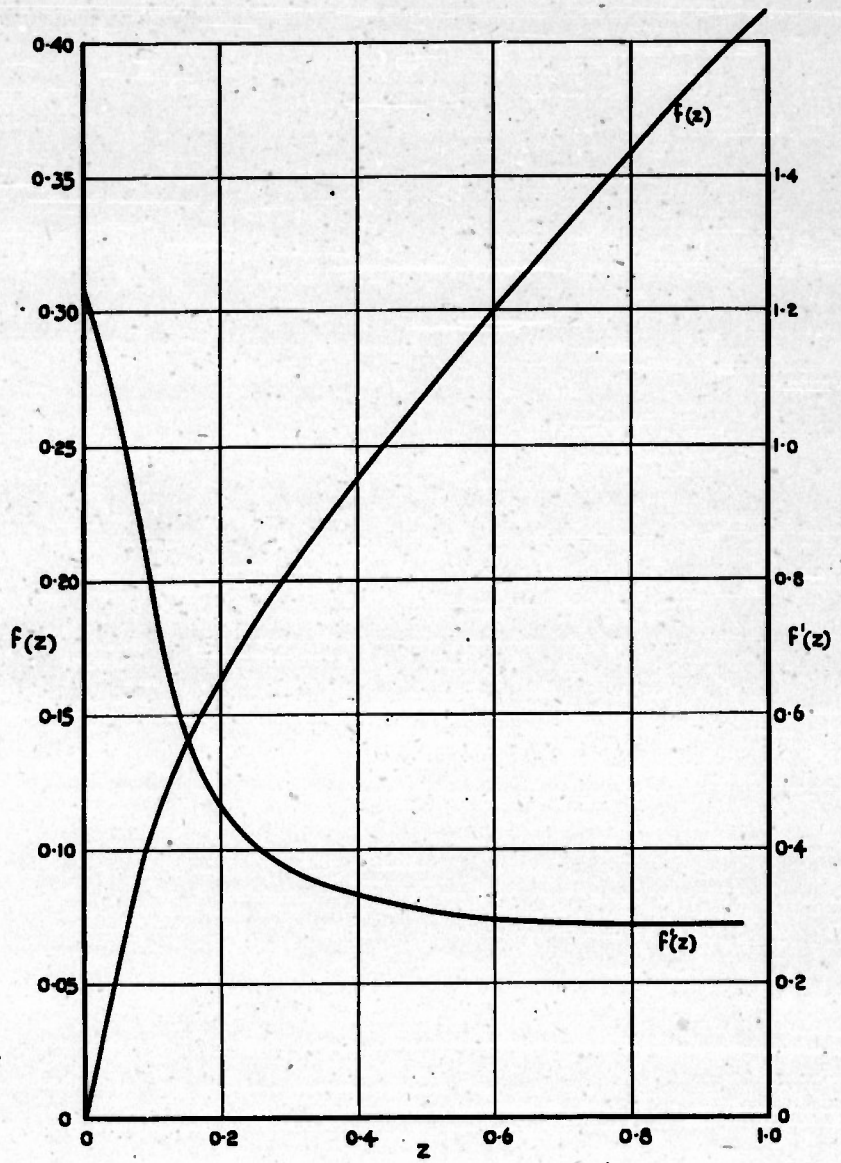


FIG. 4. VIRTUAL MASS FUNCTION.

FIG. 5

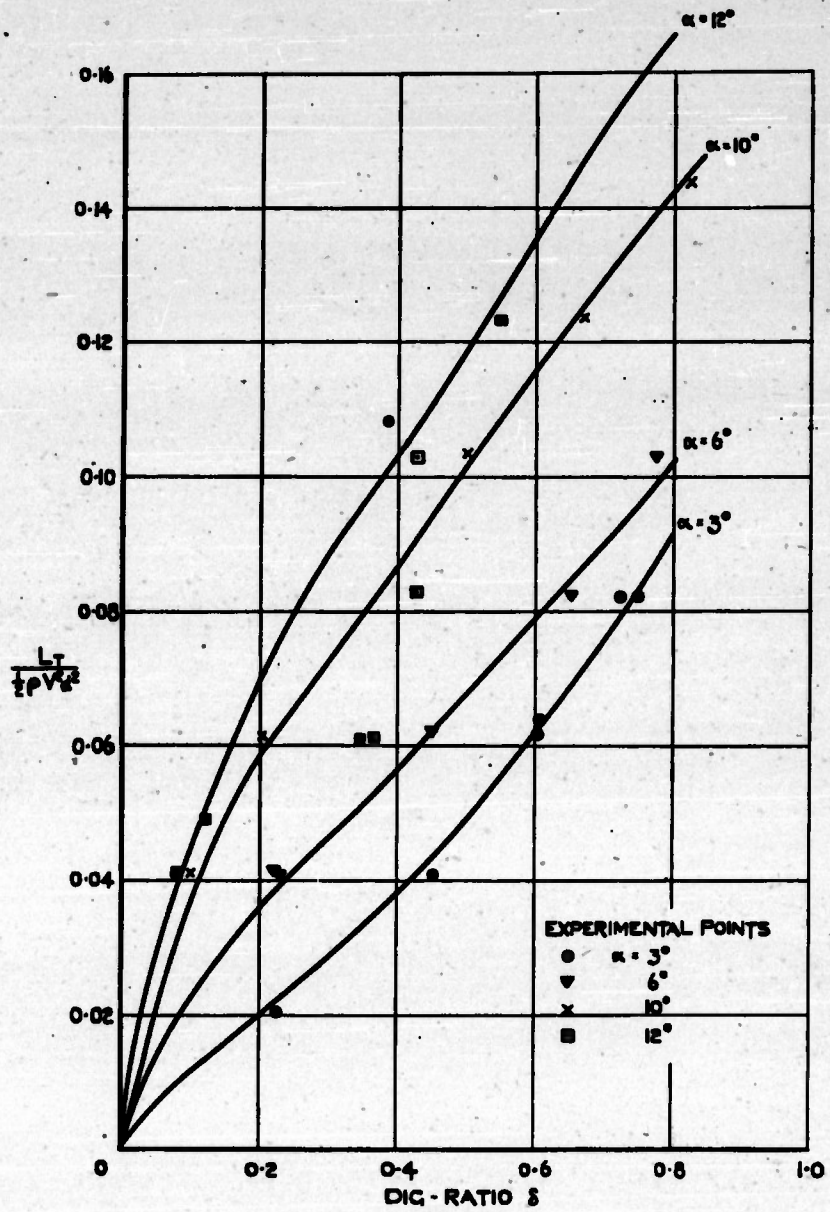


FIG. 5 COMPARISON OF THEORETICAL & EXPERIMENTAL LIFT

FIG. 6.

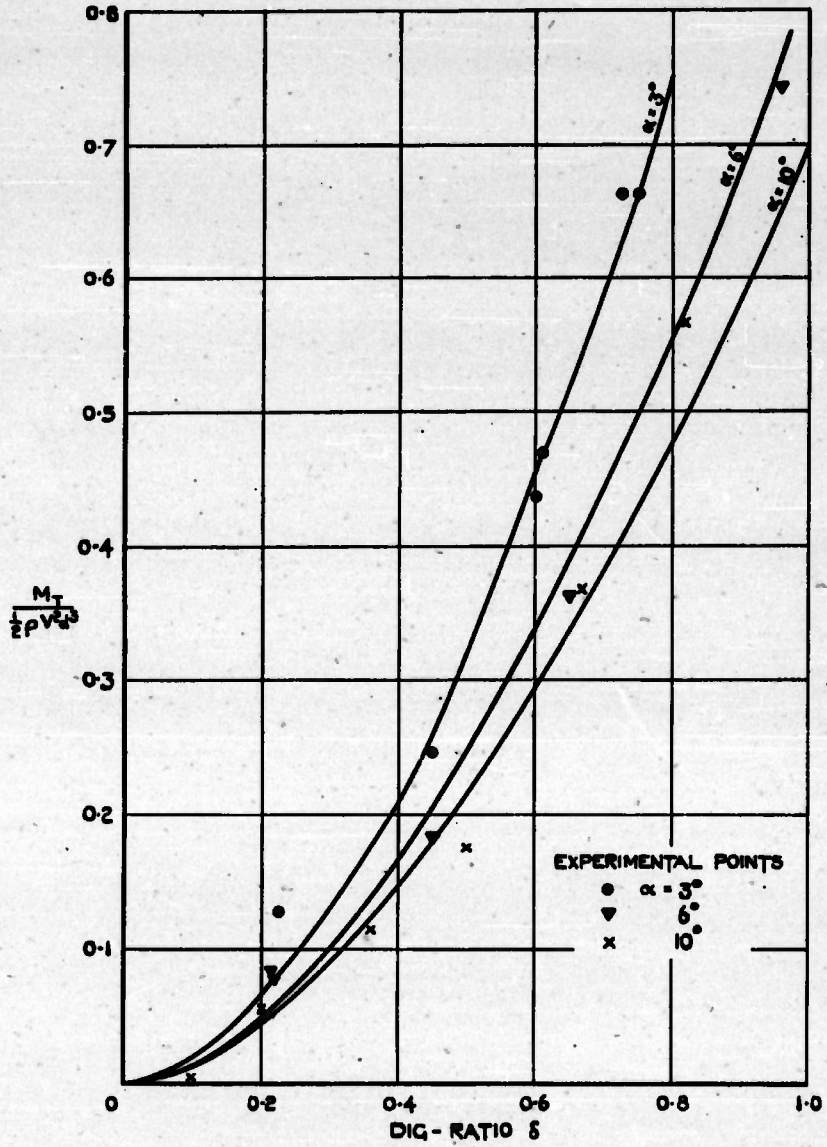


FIG. 6. COMPARISON OF THEORETICAL & EXPERIMENTAL MOMENTS.

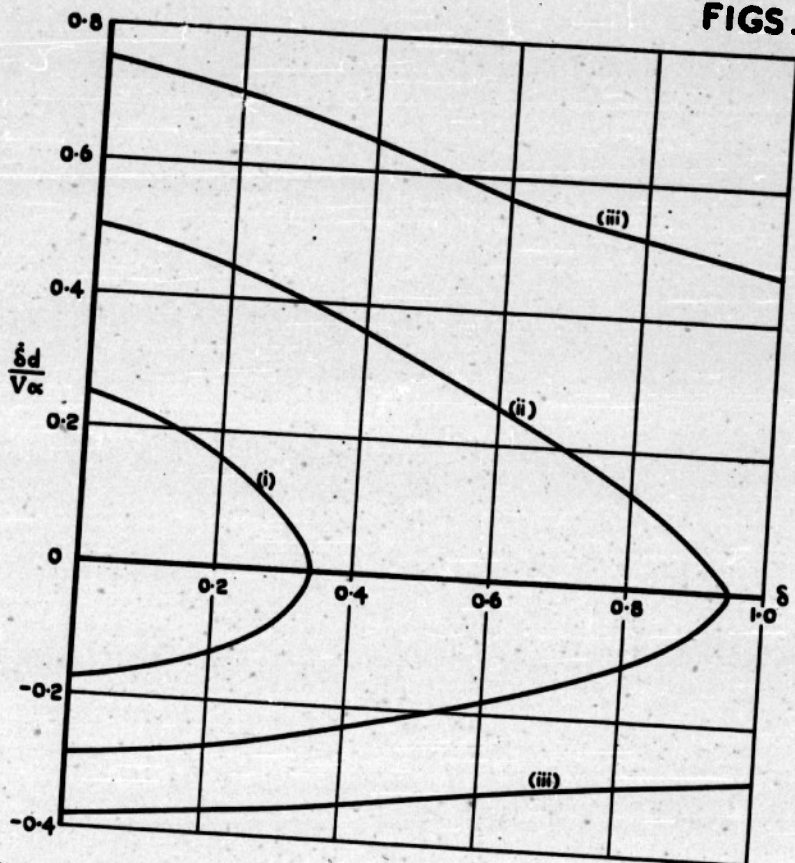


FIG. 7. OSCILLATIONS OF A PLANING CYLINDER.

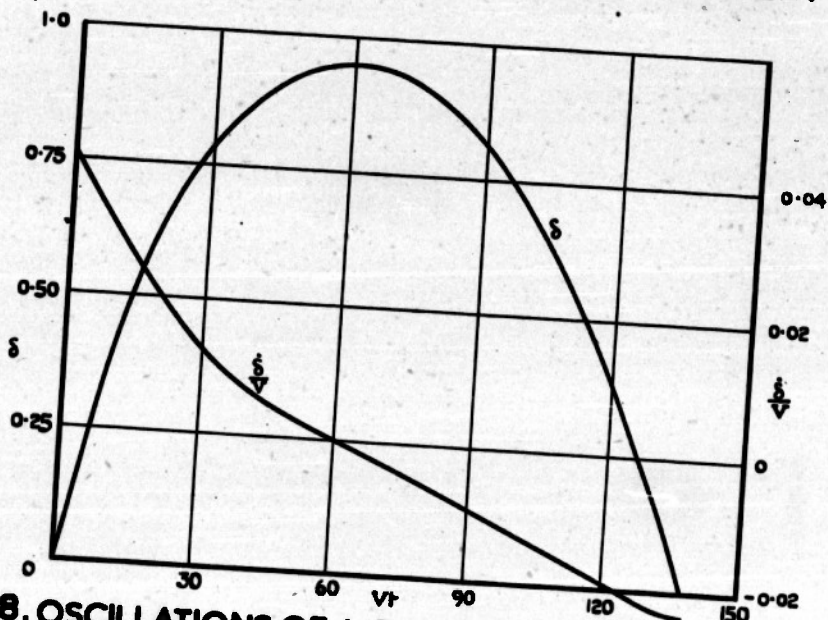


FIG. 8. OSCILLATIONS OF A PLANING CYLINDER (CASE II)

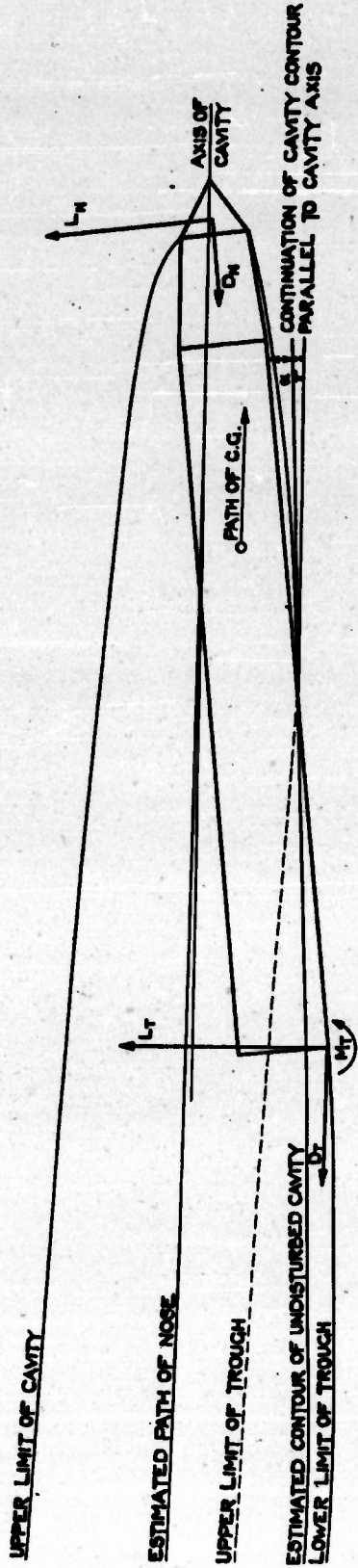


FIG. 9. FORCE SYSTEM ON A CAVITATING PROJECTILE (VERTICAL SECTION CONSTRUCTED FROM AN ACTUAL PHOTOGRAPH)

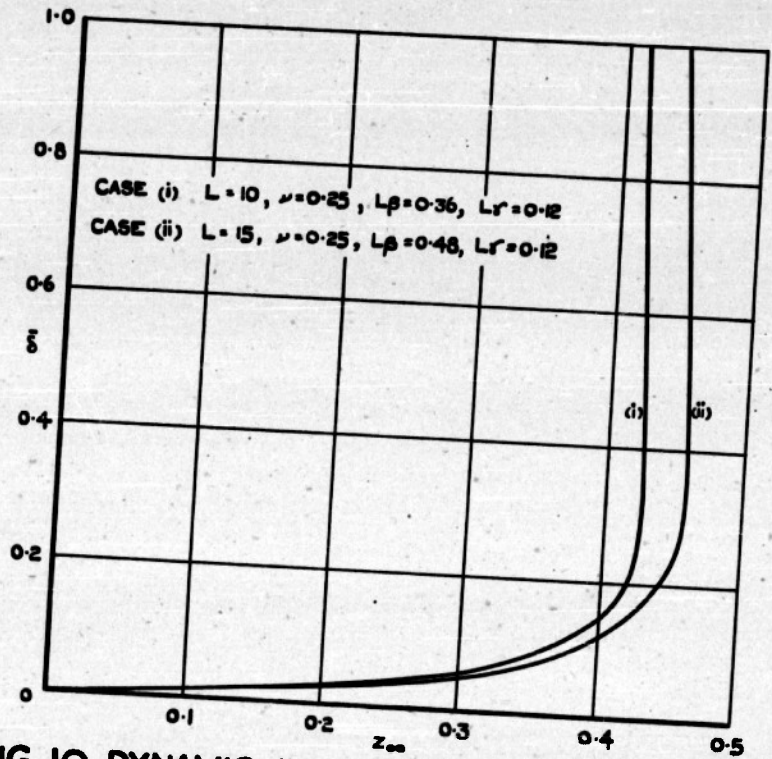


FIG. 10. DYNAMIC EQUILIBRIUM: TWO EXAMPLES

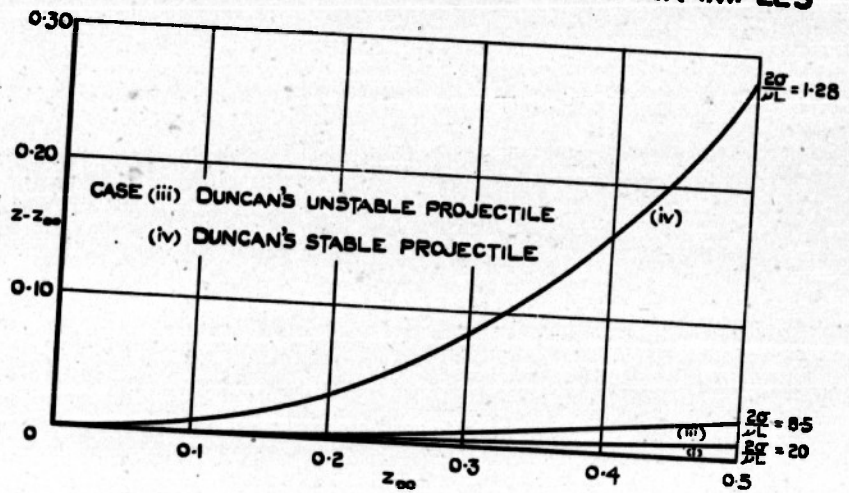


FIG. 11. DENSITY CORRECTION.

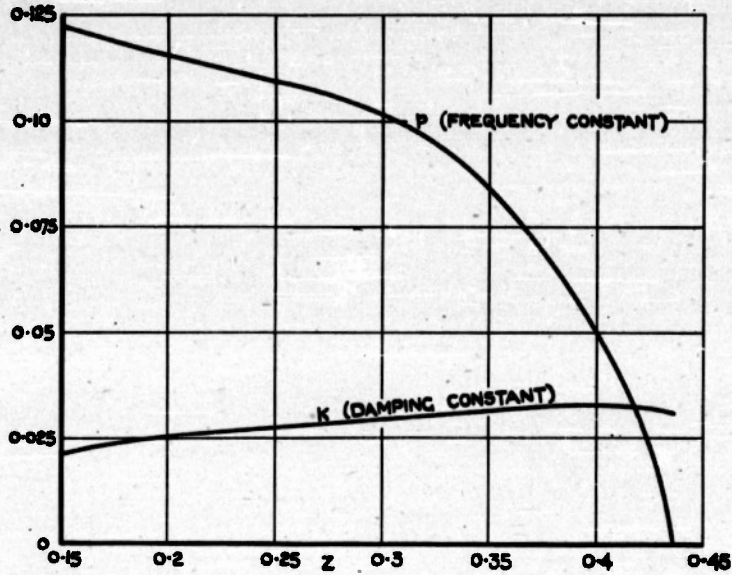


FIG. 12 DEPENDENCE OF OSCILLATIONS ON C.G. POSITION.

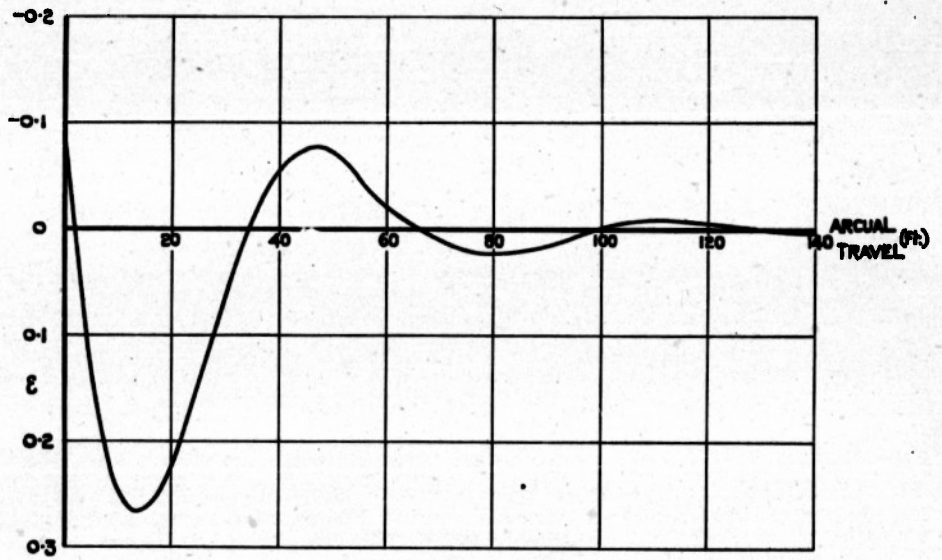


FIG. 13 OSCILLATIONS WITH A FORWARD C.G. POSITION.

FIG.14. VARIATION OF CURVATURE DURING ADJUSTMENT PHASE.

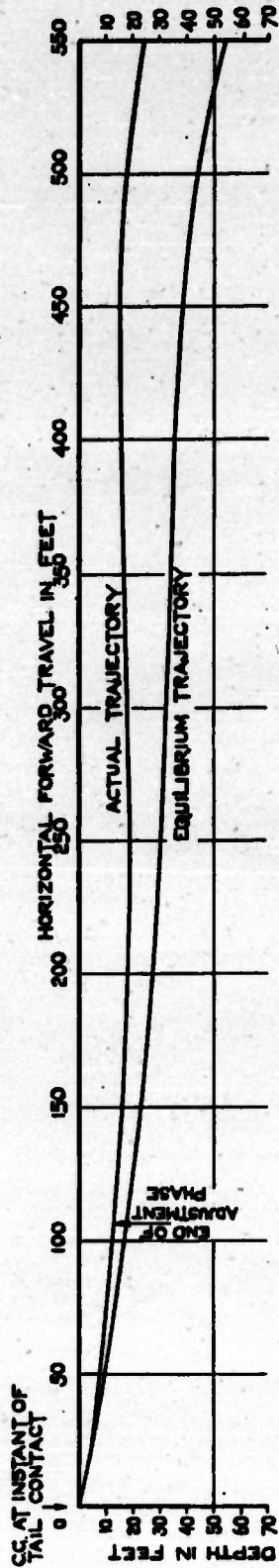
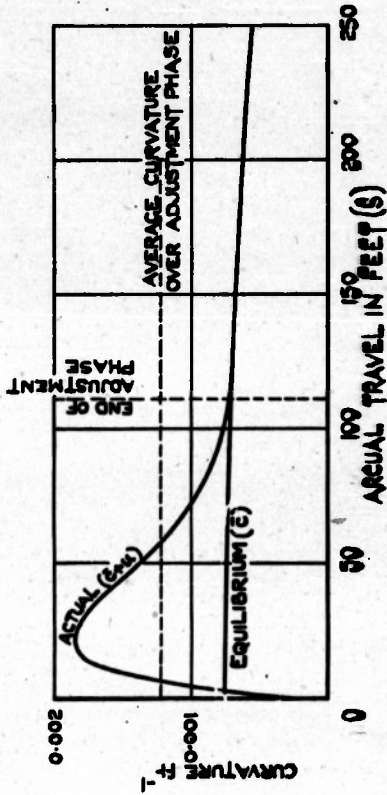
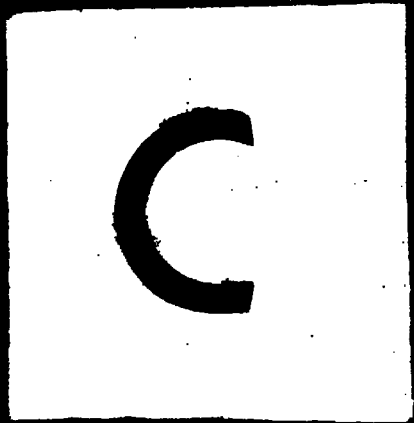


FIG.15. EQUILIBRIUM TRAJECTORY & ACTUAL TRAJECTORY.

RFFI

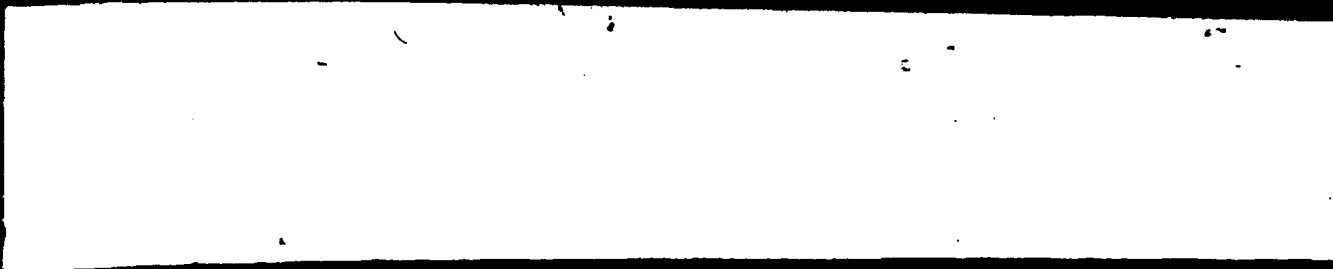


3

6

FRAME

1095



SECRET**TITLE:** The Tail Force System on Cavitating Projectiles

ATI- 1095

REVISION (None)

AUTHOR(S): Simons, N.**ORIGINATING AGENCY:** Royal Aircraft Establishment, Farnborough, HantsORIG. AGENCY NO.
TN Arm 544**PUBLISHED BY:** (Same)PUBLISHING AGENCY NO.
(Same)

DATE	SOC. CLASS.	COUNTRY	LANGUAGE	PAGES	ILLUSTRATIONS
March '46	Secr.	Gt. Brit.	Eng.	50	table, diagr, graphs

ABSTRACT:

The problems of underwater ballistics of long cavitating projectiles have been met only by a conception of steady-state motion known as "dynamic equilibrium." The technical note deals with the nonsteady motions which occur in practice and the associated variations in lift. In these phenomena, a predominant role is played by the tail forces. The development proceeds to the general motion of a cavitating projectile. The report provides a basis for future design of underwater projectiles and for the interpretation of model experiment.

DISTRIBUTION: Copies of this report obtainable from Air Documents Division; Attn: MCIDXD
DIVISION: Ordnance and Armament (22)
SECTION: Ballistics (12)

SUBJECT HEADINGS: Projectiles - Underwater ballistics
 (75420)
ATI SHEET NO.: S-22-12-5Air Documents Division, Intelligence Department
Air Materiel Command**AIR TECHNICAL INDEX****SECRET**Wright-Patterson Air Force Base
Dayton, Ohio

SECRET**TITLE:** The Tail Force System on Cavitating Projectiles**ATI-** 1095**AUTHOR(S):** Simons, N.**DIVISION** (None)**ORIGINATING AGENCY:** Royal Aircraft Establishment, Farnborough, Hants**ORIG. AGENCY NO.**
TN Arm 344**PUBLISHED BY:** (Same)**PUBLISHING AGENCY NO.**
(Same)

DATE	DOC. CLASS.	COUNTRY	LANGUAGE	PAGES	ILLUSTRATIONS
March '46	Secr.	Gt. Brit.	Eng.	50	table, diagr, graphs

ABSTRACT:

The problems of underwater ballistics of long cavitating projectiles have been met only by a conception of steady-state motion known as "dynamic equilibrium." The technical note deals with the nonsteady motions which occur in practice and the associated variations in lift. In these phenomena, a predominant role is played by the tail forces. The development proceeds to the general motion of a cavitating projectile. The report provides a basis for future design of underwater projectiles and for the interpretation of model experiment.

DISTRIBUTION: Copies of this report obtainable from Air Documents Division; Attn: MCIDXD**DIVISION:** Ordnance and Armament (22)**SECTION:** Ballistics (12)**SUBJECT HEADINGS:** Projectiles - Underwater ballistics
(75420)**ATI SHEET NO.:** S-22-12-5Air Documents Division, Intelligence Department
Air Materiel Command**AIR TECHNICAL INDEX**
SECRETWright-Patterson Air Force Base
Dayton, Ohio



*Information Centre
Technical Services
[dstl] National Library
Reference
Books
CD-ROMs
Journals
Microfilm
Video
CD-ROMs
Microfilm
Video*

Defense Technical Information Center (DTIC)
8725 John J. Kingman Road, Suit 0944
Fort Belvoir, VA 22060-6218
U.S.A.

AD#: ADA800671

Date of Search: 18 Aug 2009

Record Summary: AVIA 6/12250

Title: Tail force system on cavitating projectiles

Availability Open Document, Open Description, Normal Closure before FOI Act: 30 years

Former reference (Department) TN Arm. 344

Held by The National Archives, Kew

This document is now available at the National Archives, Kew, Surrey, United Kingdom.

DTIC has checked the National Archives Catalogue website (<http://www.nationalarchives.gov.uk>) and found the document is available and releasable to the public.

Access to UK public records is governed by statute, namely the Public Records Act, 1958, and the Public Records Act, 1967.

The document has been released under the 30 year rule.

(The vast majority of records selected for permanent preservation are made available to the public when they are 30 years old. This is commonly referred to as the 30 year rule and was established by the Public Records Act of 1967).

This document may be treated as UNLIMITED.